NASA CONTRACTOR REPORT

NASA CR-2186

NASA CR-2186

STEADY INVISCID TRANSONIC FLOWS OVER PLANAR AIRFOILS - A SEARCH FOR A SIMPLIFIED PROCEDURE

by R. Magnus and H. Yoshihara

Prepared by
GENERAL DYNAMICS/CONVAIR AEROSPACE DIVISION
San Diego, Calif.
for Ames Research Center

NATIONAL AERONAUTICS AND SPACE ADMINISTRATION • WASHINGTON, D. C. • JANUARY 1973

1. Report No.	2. Government Accession No.	3. Recipient's Catalog No.
NASA CR 2186		

4. Title and Subtitle	5. Report Date
"Steady Inviscid Transonic Flows over Planar Airfoils - A Search for a Simplified Procedure"	January 1973
	6. Performing Organization Code

7. Author(s)	8. Performing Organization Report No.
R. Magnus and H. Yoshihara	
	10. Work Unit No.

9. Performing Organization Name and Address	11. Contract or Grant No.
General Dynamics Convair Aerospace Division San Diego, California	NAS 2-6377
	13. Type of Report and Period Covered
12. Sponsoring Agency Name and Address	Contractor Report
National Aeronautics & Space Administration Washington, D.C.	14. Sponsoring Agency Code

15. Supplementary Notes

16. Abstract

Finite difference procedure based upon a system of unsteady equations in proper conservation form with either exact or small disturbance steady terms is used to calculate the steady flows over several classes of airfoils. The airfoil condition is fulfilled on a slab whose upstream extremity is a semi-circle overlaying the airfoil leading edge circle. The limitations of the small disturbance equations are demonstrated in an extreme example of a blunt-nosed, aft-cambered airfoil. The necessity of using the equations in proper conservation form to capture the shock properly is stressed. Ability of the steady relaxation procedures to capture the shock is briefly examined.

17. Key Words (Suggested by Author(s))	18. Distribution Statement
Airfoils Transonic Flow Supercritical Flow Time Dependent Method	UNCLASSIFIED-UNLIMITED

19. Security Classif. (of this report)	20. Security Classif. (of this page)	21. No. of Pages	22. Price*
Unclassified	Unclassified	57	$3.00

* For sale by the National Technical Information Service, Springfield, Virginia 22151

STEADY INVISCID TRANSONIC FLOWS OVER PLANAR AIRFOILS - A SEARCH FOR A SIMPLIFIED PROCEDURE

By R. Magnus and H. Yoshihara
General Dynamics/Convair Aerospace Division
San Diego, California

SUMMARY

A procedure to calculate steady inviscid flows over a general class of planar airfoils with embedded shocks at high subsonic Mach numbers has been developed earlier using an unsteady finite difference analogue. Here the embedded shocks were assumed to be sufficiently weak to permit the assumption of isentropic flow. The desired steady flow was obtained as the asymptotic flow for large times by prescribing suitable boundary and initial conditions. The unsteady Euler equations have been used in the proper conservation form to obtain the proper jump conditions across the embedded shock following the guidelines set forth by Lax using the concept of a weak solution to a hyperbolic initial value problem. The Lax-Wendroff two step second order difference scheme has been employed. The procedure as described above yielded satisfactory solutions for even the extreme cases of a highly blunt nosed aft cambered supercritical profiles, but at a cost of large computer times. In the present study simplifications are investigated to reduce the computer times without sacrifice of the accuracy of the solutions and always conforming to Lax's guidelines. As a first step the adequacy of the Guderley-Von Karman small disturbance theory with fictitious times derivatives and various simplified conditions at the airfoil have been examined to treat blunt nosed aft-cambered supercritical profiles. The results indicate that the simplifications are simply too severe resulting in an inacceptably poor prediction of the flow about the nose and the shock wave. A more exact formulation of the problem is then proposed where the flow domain is considered in two parts, the first sub-domain embedding the shock wave, while the second containing the remaining region where the flow is continuous. In the latter region the exact equations in non-conservation form for the two cartesian velocities are used, while the proper conservation form is employed in the sub-domain containing the shock. The exact flow tangency condition is prescribed on a semi-infinite slab where the upstream extremity is a semicircle which overlays the airfoil leading edge. Downstream of the leading edge the condition is fulfilled in a quasi-planar fashion. The procedure is

then illustrated by several examples with a supercritical profile. The report is then concluded by assessing the treatment of the embedded shocks both by the present unsteady and other steady finite difference analogues, suggesting here the need to incorporate viscous effects.

1. INTRODUCTION

In an early effort (Refs. 1-3) a finite difference procedure was developed to treat high subsonic flows with shocks over a general class of planar airfoils. Here the desired steady flow was obtained as the asymptotic flow for large times in an unsteady formulation for which a marching process could be reliably employed. The finite difference analogue here was based upon the unsteady Euler equations assuming the shocks to be sufficiently weak as to permit the assumption of isentropic flow. The airfoil condition was fulfilled exactly at the actual airfoil surface. Following the results of Lax (Ref. 4) the equations were used in an appropriate conservation form to insure jump conditions corresponding to the isentropic limit of the Rankine-Hugoniot conditions. As a consequence of the dissipation generated by the truncation errors, the shock discontinuities were endowed with a profile (to be sure a fictitious one), so that the flow could then be treated as entirely continuous. Of course, a fine mesh must be employed about the shocks to obtain an adequate spacial resolution of the shocks and to minimize the extent of the inadmissible region within the shock profile. Embedded shocks were thus evolved automatically in the analogue, a liability (truncation error) here being parlayed to resolve the very difficult task of treating the a priori unknown embedded shocks - a rare event indeed especially in transonic aerodynamics. A drawback of these early efforts was the resulting complexity, in particular in the fulfillment of the boundary condition at the airfoil, which led to a large expenditure of computer time. The emphasis at this early stage was concentrated in obtaining meaningful results, and this preoccupation compounded by the conservatism engendered by the lack of both experience and resources resulted in a procedure, which, in light of progress to date, must now be considered obsolete. Thus the goal of the present effort is a thorough renovation of the above unsteady procedure to reduce the computer costs without significantly compromising the accuracy and the generality of flows that can be treated. At the same time the resulting numerical procedure must be suitable for use in an overall procedure to incorporate viscous effects, and for ultimate extension to steady three dimensional flows. The retainment of the unsteady format here to treat steady flows was motivated to be sure by our past experience, but more so by the firm foundation on which the unsteady analogue rests, namely in the treatment of

shocks via the concept of weak solutions developed by Lax (Ref. 4). A real unsteady approach would, of course, also fill a dire need for a procedure to treat supercritical unsteady flows.

Subsequent to the introduction of the above unsteady analogue there has been phenomenal progress in the development of steady finite difference procedures using relaxation techniques that has reduced the problem of large computer times. The key to this progress was the introduction by Murman and Cole (Ref. 5) of a finite difference scheme that was locally tailored to be compatible with the local domain of dependence, and the use of a line relaxation in a direction natural to near-sonic flows. In their efforts the transonic small perturbation equation of Guderley and Von Karman was used together with planar boundary conditions. The basis of subsequent more exact procedures of Lomax and Steger (Ref. 6) and Garabedian and Korn (Ref. 7) have been centered on the above innovations of Murman and Cole. (These procedures are reviewed in Ref. 8). Despite the ostensible success of the above steady analogues, there are some apparent shortcomings in the treatment of the shocks that are difficult to assess fully due to the absence of a guiding background comparable to Lax's contributions for the hyperbolic unsteady case.

In Section 2 to follow we shall first as a review formulate the problem starting with the exact unsteady non-isentropic case, followed by the Guderley-Von Karman unsteady small disturbance case, and the small disturbance and exact cases with fictitious time derivatives. The intent here, in order, is to introduce the use of the concept of the weak solution by Lax to justify heuristically the use of the unsteady analogue to treat flows with shock discontinuities, to review the consequences of the small disturbance limiting process to clarify the compatibility of shock pressure drag with the isentropic state of the flow, and finally to introduce the use of fictitious time derivatives to advantage when the sole interest is in the steady flows. In Section 3 factors in the formulation of the problem and in its numerical analogue which affect computer costs, will be discussed briefly, while in Section 4 some results using the simple equations and boundary conditions will be described for the severe case of a highly blunt-nosed, aft-cambered profile representative of the supercritical profiles now receiving extensive attention. In Section 5 we shall next describe the procedure proposed to meet the objectives listed earlier, and illustrate its use for a case with a "peaky" supercritical airfoil. In the concluding remarks we shall review and assess the treatment of the shock discontinuities by both the steady and unsteady finite difference analogues, (in this connection the role of Zierep's local analysis about the "foot of the shock" will be related); finally followed by a discussion stressing the need to incorporate the viscous effects.

2. Formulation of the Airfoil Problem

We are concerned with flows over a general class of profiles at high subsonic Mach number M_∞ in which one or more embedded shock discontinuities may arise. The flow thus is to be considered inviscid everywhere except at the shock discontinuities where the flow particles are assumed to suffer an abrupt increase in entropy as they pass through the shock. The flow is assumed to be non-heat conducting everywhere including the shock so that any heat additions by dissipation within a fluid particle is confined to that particle; that is, the flow will be everywhere adiabatic. The flow will be additionally isentropic (and therefore irrotational) at all points except in the subdomain downstream of the shock discontinuities, where the flow will be non-isentropic and therefore rotational when the shock is of variable strength or curved in shape. Downstream of the shock the entropy will be constant along any given streamline, but will in general differ from streamline to streamline.

Under these conditions the basic flow equations in cartesian coordinates are given by

$$\frac{\partial W}{\partial t} + \frac{\partial F}{\partial x} + \frac{\partial G}{\partial y} = 0 \tag{1}$$

where the vectors W, F and G are given by

$$W = \begin{Bmatrix} \rho \\ \rho u \\ \rho v \\ \rho\left[\frac{1}{2}(u^2 + v^2) + e\right] \end{Bmatrix}$$

$$F = \begin{Bmatrix} \rho u \\ \rho u^2 + p \\ \rho uv \\ \rho u\left[\frac{1}{2}(u^2 + v^2) + h\right] \end{Bmatrix} \qquad G = \begin{Bmatrix} \rho v \\ \rho uv \\ \rho v^2 + p \\ \rho v\left[\frac{1}{2}(u^2 + v^2) + h\right] \end{Bmatrix}$$

When the equations are given in the divergenceless form of Eq. (1), it is said to be in conservation form. In the above the usual symbols have been employed with the less familiar symbols h and e noting respectively the specific enthalpy and specific internal energy. For ideal diatomic gases the specific enthalpy is defined and given by

$$h \equiv e + \frac{p}{\rho} = \frac{\gamma}{\gamma - 1} \frac{p}{\rho} \tag{2}$$

while the specific internal energy e is given by

$$e \equiv c_v T = \frac{1}{\gamma - 1} \frac{p}{\rho} \tag{3}$$

Here c_v is the specific heat at constant volume, γ is the ratio of specific heats equal to 1.4 for air, and T is the absolute temperature. With the value of h and e from Eqs. (2) and (3) inserted in (1), the resulting equations form a fully determined set of four equations for the four unknowns p, ρ, u, and v. A further useful thermodynamic relation, the caloric equation of state, which is in fact implied in Eqs. (2) and (3) is given by

$$p = \rho RT = \rho^{\gamma}(\gamma - 1) \exp\left(\frac{S - S_o}{c_v}\right) \tag{4}$$

where $R = c_p - c_v$ is the gas constant, S is the entropy, and S_o is a constant reference value.

Across the shock discontinuities we must additionally fulfill the shock jump conditions representing the conservation of mass, momentum, and energy. Thus in general for a moving shock with N_S the component of the shock velocity normal to the shock, we have

$$\rho_1(N_1 - N_S) = \rho_2(N_2 - N_S) \qquad \text{(mass)}$$

$$\rho_1 N_1(N_1 - N_S) + p_1 = \rho_2 N_2(N_2 - N_S) + p_2 \qquad \text{(momentum)}$$

$$T_1 = T_2 \qquad \text{(momentum)} \tag{5}$$

$$\frac{1}{2}\rho_1(N_1 - N_S)(N_1^2 + T_1^2) + \rho_1(N_1 - N_S) e_1 + N_1 p_1 \qquad \text{(energy)}$$

$$= \frac{1}{2}\rho_2(N_2 - N_S)(N_2^2 + T_2^2) + \rho_2(N_2 - N_S) e_2 + N_2 p_2 \ .$$

Here N and T are respectively the velocity components normal and tangent to the shock front, and the subscripts 1 and 2 denote conditions upstream and downstream of the shock. (See Sketch A).

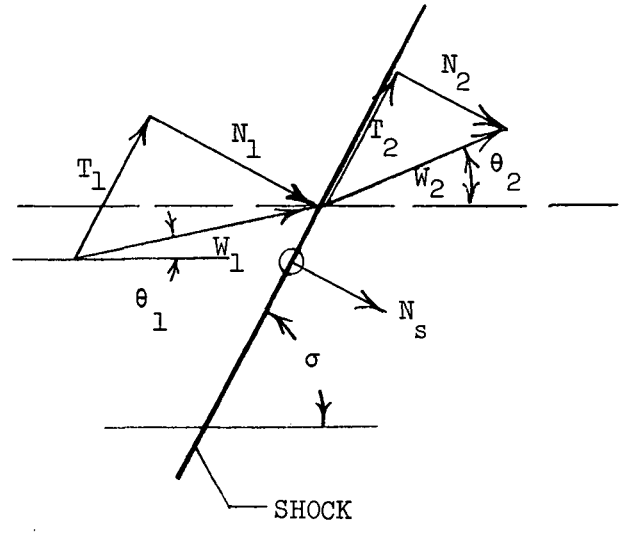

Sketch A. The Oblique Shock Nomenclature

In addition to the jump conditions (5) we must additionally impose the condition

$$S_2 \geq S_1 \tag{6}$$

where the entropy S is defined in (4).

The jump conditions (5) can be expressed in terms of the cartesian velocity components by using the following correspondence:

$$\frac{N_i}{W_i} = \sin(\sigma - \theta_i) \qquad i = 1, 2$$

$$\frac{T_i}{W_i} = \cos(\sigma - \theta_i)$$

where

$$W_i^2 = u_i^2 + v_i^2$$

$$\tan \theta_i = \frac{v_i}{u_i}$$

and σ is slope of the shock relative to the freestream direction. We note here for future use the well-known result that the change of entropy $S_2 - S_1$ across the shock is third order in terms of the shock strength defined, for example, as the difference of the pressures $p_2 - p_1$ across the shock. Finally we recall that for a steady adiabatic, but non-isentropic flow an integral of the flow equations, the strong Bernoulli law, exists valid along a streamline given by

$$h + \frac{1}{2} q^2 = \frac{1}{2} q_L^2 \tag{7}$$

where $q^2 = u^2 + v^2$, and q_L is the limit speed obtained by expanding the gas isentropically to a vacuum. The value of the limit speed q_L will in this case be constant along a given streamline but will vary from streamline to streamline in accordance to the equation

$$\text{grad } \frac{1}{2} q_L^2 = T \text{ grad } S + \vec{q} \times \text{curl } \vec{q}$$

where $\bar{q}$ is the velocity vector. Further with the use of Eq. (2), Eq. (7) can be rewritten as

$$p = \frac{\gamma - 1}{2\gamma} \rho(q_L^2 - q^2) \tag{8}$$

We shall use this expression later to eliminate p for an isentropic case where q_L is a constant.

Consider next the formulation of the boundary and initial conditions to supplement the differential equations (1) for the singly connected domain G as enclosed by the boundary C of Sketch B.

Here the outer boundary ABC is taken sufficiently far from the airfoil that the freestream conditions can be prescribed on this contour for all times.

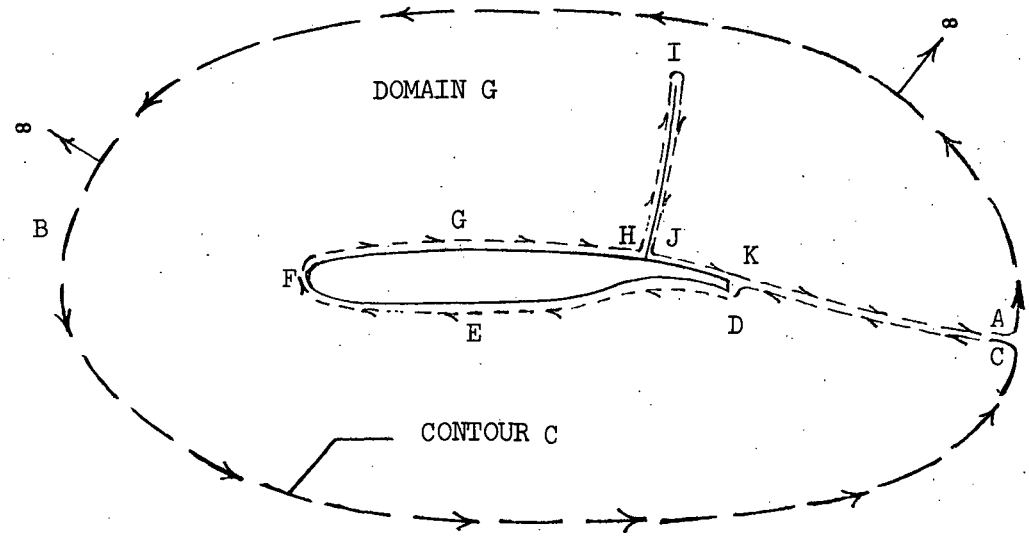

Sketch B. Domain of the Problem

At the surface of the body $y = y_B(x)$ for $t \geq 0$ we require the flow tangency requirement

$$\frac{v(x, y_B)}{u(x, y_B)} = y_B'(x). \tag{9}$$

(Note that $y_B(x)$ must be a double valued function of x, the two branches corresponding to the upper and lower surfaces.) At the airfoil trailing edge we must fulfill the Kutta condition requiring the equality of pressures at K and D for $t \geq 0$. For an unsteady case where the lift is changing with time, the rear stagnation streamline will be a vortex sheet (contact surface), so that for $t \geq 0$ we must fulfill the jump conditions that at corresponding points along KA and DC the pressure and the flow direction must be equal. As the steady state is reached, of course, the vortex sheet disappears; and the flow becomes continuous across the rear stagnation streamline. At corresponding points on either side of the shock, HI and IJ, one must fulfill the shock jump conditions given earlier in Eqs. (5) and (6). Finally at a given time $t = t_o < 0$ we must prescribe the initial values of the dependent variables at all points of G. This initial flow need not fulfill any of the above boundary conditions, and an uniform flow at the freestream conditions or an available neighboring flow is generally used.

The flow in domain G is entirely continuous, so that the flow equations may be used in any appropriate form; in particular, they need not be used in the conservation form given in Eq. (1). The difficulty of the above choice of

the domain G is that the location of the shocks is not known beforehand, or if it is known at the initial time, a procedure must then be incorporated to determine the shock locations at all later times, clearly a difficult task. A procedure based upon this approach was in fact devised ingeneously by Grossmann and Moretti (Ref. 9) who treated several simple cases. In the present study, we shall circumvent the task of having to determine the instantaneous shock locations by redefining the inner boundary of Sketch B such that it lies adjacent to the airfoil surface and does not exclude the shocks. The flow domain defined by such a boundary will now contain flow (shock) discontinuities, and the dependent variables and their first partial derivatives will no longer be continuous, but will be piecewise continuous. In such a situation derivatives can no longer be defined at the shock discontinuities making it impossible to check the fulfillment of the equations. To circumvent this difficulty Lax (Ref. 4) used a generalization of the concept of a solution, the so-called weak solution, which we shall briefly review in the next sub-section.

2.1 Weak Solutions. (See Courant-Hilbert, Ref. 10)

To handle solutions of first order quasi-linear hyperbolic equations which are piecewise continuous, and possess piecewise continuous first derivatives, the concept of the weak solution was introduced by Lax (Ref. 4). Thus consider the simple case of Eq. (1) in two dimensions

$$W_t + F_x = 0 \tag{10}$$

Instead of requiring this equation to be fulfilled, a "weaker" requirement on the "solution" is imposed given by the equation

$$\iint_R \zeta (W_t + F_x)\, dx\, dt = 0 \tag{11}$$

where R are subdomains of G (the flow domain), and ζ are arbitrary "test vectors" having a certain required smoothness and vanishing outside of R. First for subdomains R not containing a shock discontinuity Eq. (11) reduces to (10), and the usual solution, the genuine solution, is obtained. For subdomains containing a shock Eq. (11) will be rewritten as

$$\begin{aligned} \iint_R \zeta [W_t + F_x]\, dx\, dt = & \iint_R [(\zeta W)_t + (\zeta F)_x]\, dx\, dt \\ & - \iint_R (W\zeta_t + F\zeta_x)\, dx\, dt = 0 \end{aligned} \tag{12}$$

The first integral on the right side may be reduced to a contour integral using Green's formula with the result

$$\iint_R [(\zeta W)_t + (\zeta F)_x]\, dx\, dt = \oint_s \zeta[W dx - F dt] \tag{13}$$

where s is the contour enclosing R. If we next use instead a contour equivalent to s shown in Sketch C, and the fact that $\zeta = 0$ along those segments of the alternate contour not "wetting" the shock, we can rewrite (13) as

$$\iint_R [(\zeta W)_t + (\zeta F)_x]\, dx\, dt = \int_{\text{shock}} \zeta \left\{ [W] \left.\frac{dx}{ds}\right|_{\text{shock}} - [F] \left.\frac{dt}{ds}\right|_{\text{shock}} \right\} ds \tag{14}$$

where ds is a line element along the shock, $[W] \equiv W_1 - W_2$ and $[F] = F_1 - F_2$ (subscripts 1 and 2 denoting conditions upstream and downstream of the shock), and $\left.\frac{dx}{ds}\right|_{\text{shock}}$ and $\left.\frac{dt}{ds}\right|_{\text{shock}}$ are the direction cosines of the shock.

Eq. (12) using Eq. (14) now becomes

$$\iint_R (W\zeta_t + F\zeta_x)\, dx\, dt - \int_{\text{shock}} \zeta \left\{ [W] \left.\frac{dx}{ds}\right|_{\text{shock}} - [F] \left.\frac{dt}{ds}\right|_{\text{shock}} \right\} ds = 0 . \tag{15}$$

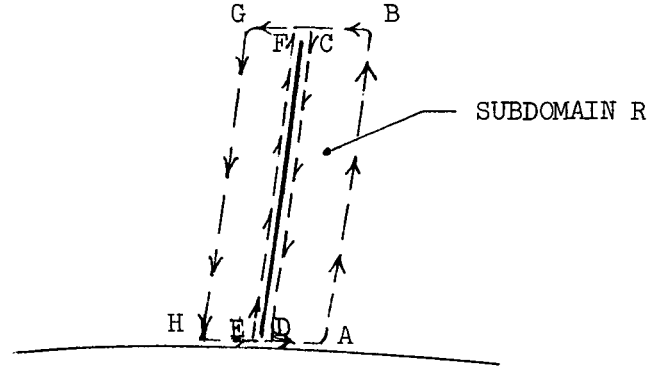

ORIGINAL CONTOUR FOR R: ABGHA

REVISED CONTOUR: ABCDEFGHA

Sketch C. Revised Contours for the Weak Solution

We now define a weak solution W (or F) of (10) if it is piecewise continuous with piecewise continuous first derivatives, and if it fulfills the equation

$$\int\int (W\zeta_t + F\zeta_x)\, dx\, dt = 0 \tag{16}$$

for all admissible "test vectors" ζ in all subdomains R within the flow domain G. From (15) with (16) fulfilled, it follows that weak solutions will fulfill the condition

$$\int_{\text{shock}} \zeta \left\{ [W] \left.\frac{dx}{ds}\right|_{\text{shock}} - [F] \left.\frac{dt}{ds}\right|_{\text{shock}} \right\} ds = 0 \tag{17}$$

Since ζ is an arbitrary "test vector", for Eq. (17) to be fulfilled we must require

$$[W] \left.\frac{dx}{ds}\right|_{\text{shock}} - [F] \left.\frac{dt}{ds}\right|_{\text{shock}} = 0 \tag{18}$$

which is, without surprise, the unsteady one dimensional shock jump conditions. Thus a weak solution as defined above will fulfill the correct jump conditions across embedded shocks. The definition of weak solutions as given above can be extended to higher space dimensions. (See Ref. 10). Weak solutions as defined above have some surprising properties, and these are described by Lax in Ref. 4. Two of these are of particular relevance to us. The first is the fact that the shock jump conditions will depend upon the specific conservation form of the basic flow equations used as would be expected by inspection of Eq. (18). Thus it is essential that the basic flow equations be used only in the form given in Eq. (1) for subdomains containing a shock. The second property is that for an initial value problem, the initial data alone do not determine an unique solution. A supplementary condition must be additionally imposed, but the nature of the additional condition is known unfortunately only for a few simple initial value problems. In a number of these simple cases with a first order quasi-linear hyperbolic equation where the exact analytical solution is known, it has been shown analytically using (16) that an unique weak solution was obtained as the limiting solution (viscosity$\to$0) of a corresponding viscous problem where an artificial viscous term was added to the original equation. Further Lax has shown that for the same problem the same weak solution was essentially obtained as a limiting solution for small mesh using an appropriate finite difference analogue. This is a fortunate result, though not altogether surprising, since an artificial viscosity is also implied in the first order diffusing difference scheme used by Lax.

For the hyperbolic combined initial-boundary value problem of higher dimension of interest to us, we have no direct prior analysis to guide us as in the simpler cases; we must extrapolate the conclusions from the simpler cases studied by Lax and others, and indeed we must be grateful that such information is available, since it does offer a reasonably sound point of departure. Thus we may conclude that a reasonable procedure for the airfoil problem is to pose it as a hyperbolic initial-boundary value problem using the equations in an appropriate conservation form and then solving it by an appropriate finite difference analogue. In such a procedure the correct shock jump conditions can be expected to be fulfilled across the embedded shocks. It is essential here that in subdomains containing a shock discontinuity, the proper conservation form of the equations be used. Lax (Ref. 4) and Ref. 11 have shown that for the one dimensional unsteady shock wave problems when the equations are used in the non-conservation form, either the wrong shock speed results when the shock is moving, or the required jump conditions are not fulfilled when the shock is stationary. In passing one should finally note that a comparable background and point of departure does not exist in the steady finite difference analogues.

2.2 Guderley-Von Karman Formulation of the Problem (See Guderley, Ref. 12)

We need not dwell at length on the transonic small disturbance theory except to recall that it is the result of a very definite limiting process $\tau \to 0$ carried out in the basic equations (1) using the transformation (hypothesis)

$$\begin{aligned} u(x,y,t) &= a^*[1 + \tau\, \tilde{u}(\xi,\eta,\tilde{t})] \\ v(x,y,t) &= a^*\, \tau^{3/2}\, \tilde{v}(\xi,\eta,\tilde{t}) \\ p(x,y,t) &= p^*[1 + \tau^{3/2}\, \tilde{p}(\xi,\eta,\tilde{t})] \\ \rho(x,y,t) &= \rho^*[1 + \tau^{3/2}\, \tilde{\rho}(\xi,\eta,\tilde{t})] \end{aligned} \tag{19}$$

where

$$\xi = \frac{x}{x_o}\,, \qquad \eta = \tau^{1/2}\,\frac{y}{x_o}\,, \qquad \tilde{t} = \omega t\,.$$

For a limit of ω representing reduced frequencies of order unity, the resulting limiting equations (lowest order in τ) are found to be

$$\tilde{u}_{\tilde{t}} = -(\gamma + 1)\,\tilde{u}\,\tilde{u}_{\xi} + \tilde{v}_{\eta} \quad ; \qquad 0 = \tilde{u}_{\eta} - \tilde{v}_{\xi}\,. \tag{20}$$

Applying (19) to the airfoil boundary condition, one obtains the standard planar condition $\tilde{v}(\xi \pm 0) = h^{\pm}(\xi)$ where $h^{\pm}(\xi)$ are the slopes on the upper and lower sides of the profile for the stretched coordinates. There is much implied in Eq. (19), and in particular the various powers of τ have of course been selected here, so that the resulting lowest order equations and the coordinate stretching would be physically viable. The parameter τ (proportional to the airfoil thickness ratio to the two-thirds power) is a measure of the proximity of the flow velocities to the sonic speed, so that the limiting process $\tau \to 0$ implies values of M_∞ close to one and thin airfoils at small incidences. It is particularly interesting that in this limit the flow is irrotational and hence isentropic. This should not be surprising since the pressure coefficient $C_p \equiv \frac{p - p^*}{q^*}$ is first order in τ, while the entropy change across the shock is third order in the shock strength, or $O(\tau^3)$.

The order of magnitude assessment of the various terms in the flow equations solely in terms of powers of τ can be misleading since the actual magnitude of a term in fact depends additionally on the algebraic magnitude of the term itself. Thus in an unfavorable situation it may require such a small value of τ for the above small disturbance theory to be valid, that the resulting flow would be of no practical value.

Lastly, it should be noted that the unsteady Guderley-Von Karman equations as given in Eq. (20) are of mixed parabolic-hyperbolic type, so that Lax's concept of weak solutions does not apply directly to these equations. If we are interested only in the steady state, fictitious fully hyperbolic equations can be obtained by introducing appropriate unphysical time derivatives, and we shall examine this in the next sub-section.

2.3 Fictitious Unsteady Equations to Treat Steady Flows

In preparation for Sections 4-5 in the present sub-section we shall simply note several sets of equations all under isentropic conditions, having fictitious time derivatives which result in fully hyperbolic systems when added to either the Guderley-Von Karman or the exact steady terms. Thus for the small disturbance case we have

$$\tilde{u}_{\tilde{t}} = -(\gamma + 1)\left(\frac{1}{2}\tilde{u}^2\right)_\xi + (\tilde{v})_\eta \quad ; \quad \tilde{v}_{\tilde{t}} = \tilde{u}_\eta - \tilde{v}_\xi \quad ; \tag{21}$$

or with the exact steady terms (in non-conservation form)

$$u_t = (a^2 - u^2)\, u_x - 2uv\, u_y + (a^2 - v^2)\, v_y$$

$$v_t = u_y - v_x \tag{22a}$$

where the speed of sound is given by

$$a^2 = \frac{1}{2}(\gamma + 1)\, a^{*2} - \frac{1}{2}(\gamma - 1)\, (u^2 + v^2)$$

Eq. (22a) can be also rewritten in a conservation form

$$u_t = (\rho u)_x + (\rho v)_y$$

$$v_t = - v_x + u_y \tag{22b}$$

where $\rho = \rho(u, v)$ from the isentropic relation.

It is to be noted that these equations are not in the proper conservation form that yields the correct shock jump conditions, and its use should be restricted to subdomains where the flow is continuous.

Lastly we note for subsequent use the exact unsteady Euler equations in the proper conservation form obtained from the Eqs. (1) for the isentropic case, that is,

$$\frac{\partial}{\partial t} \begin{Bmatrix} \rho \\ \rho u \\ \rho v \end{Bmatrix} + \frac{\partial}{\partial x} \begin{Bmatrix} \rho u \\ \rho u^2 + p \\ \rho uv \end{Bmatrix} + \frac{\partial}{\partial y} \begin{Bmatrix} \rho v \\ \rho uv \\ \rho v^2 + p \end{Bmatrix} = 0 \tag{23}$$

where

$$\frac{p}{p^*} = \left(\frac{\rho}{\rho^*}\right)^{\gamma} = \frac{\gamma - 1}{2\gamma} \frac{\rho}{p^*} (q_L^2 - q^2)$$

Shock jump conditions for the asymptotic steady state for the above hyperbolic equations can be obtained using Eq. (18) extended to the unsteady planar flow case. Thus for the small disturbance equations we obtain the jump conditions

$$\left[-\frac{1}{2}(\gamma+1)\,\tilde{u}^2\right]\left.\frac{dy}{dx}\right|_{shock} - [\tilde{v}] = 0$$

$$[\tilde{v}]\left.\frac{dy}{dx}\right|_{shock} + [\tilde{u}] = 0$$

Here again the brackets [ ] denote a jump of the bracketed quantity across the shock. Thus for a normal shock adjacent to the airfoil surface, where $[\tilde{v}] \equiv 0$ in accordance to the planar airfoil condition, we have $[\tilde{u}^2] = \tilde{u}_1^2 - \tilde{u}_2^2 = 0$, or $\tilde{u}_1 = -\tilde{u}_2$, since $\tilde{u}_1 \neq \tilde{u}_2$.

Such a condition conforms to the transonic shock polar only if $\tilde{v}_1 \sim 0$, that is for shock waves essentially normal to the free stream. In the planar case if the basic small disturbance restrictions are not violated, shock waves that depart from a normality with the free stream cannot arise, so that the shock captured by the small disturbance weak solution will automatically conform to the consistent shock polar. The same situation would prevail also for the three dimensional case described by the usual small disturbance equations, where again shock jump conditions implied by the weak solution will not conform to the appropriate shock polar if the shocks are not essentially normal to the unperturbed basic flow direction. Thus if an excessive wing sweep causes an excessively swept shock (sweep of 25° is excessive), then the small disturbance jump conditions would not be fulfilled for such shocks. (Excessive sweep effects have of course never been permitted by the small disturbance hypothesis.)

Lastly we note that the shock jump conditions for the exact equations (23) in the asymptotic steady state are given by

$$\begin{bmatrix} \rho u \\ \rho u^2 + p \\ \rho uv \end{bmatrix} \left.\frac{dy}{dx}\right|_{shock} - \begin{bmatrix} \rho v \\ \rho uv \\ \rho v^2 + p \end{bmatrix} = 0$$

which after some algebraic manipulations can be shown to agree with the Rankine-Hugoniot conditions given earlier in Eq. (5) with the shock speed set equal to zero.

2.4 The Paradox of Isentropic Transonic Wave Drag

It is universally accepted that the onset of transonic wave drag over airfoils in an inviscid flow for $M_\infty < 1$ is the consequence of streamwise momentum loss in the far field due to entropy additions by shock waves. The question then

naturally arises as to how a drag can arise if an isentropic flow is assumed. To answer this let us consider the determination of the drag by the vanishing of the flux of the total streamwise momentum (including the pressure term) through the control surface of Sketch B. Consider the case that the flow is calculated with the exact non-isentropic equations with the shocks treated either as discontinuities fulfilling the Rankine-Hugoniot jump conditions, or evolved by the continuous shock-capturing weak solution to the appropriate conservation equations. Vanishing of the streamwise momentum flux through the contour C (Sketch B) then yields the equivalence of the airfoil drag with the deficiency of the streamwise momentum flux through the far downstream portion of the contour, since the momentum is conserved across the shock. Since this far field momentum deficiency can be directly attributed to the increase in entropy, in the exact non-isentropic case the drag is indeed the consequence of the shock entropy additions. If we now calculate the flow in the same manner but using instead the exact isentropic equations and evaluate the total momentum along the control surface, we find that the momentum flux deficiency along the far downstream boundary vanishes identically, and the drag is now equal to the change of the streamwise momentum flux across the shock wave. If the equations are used in the proper conservation form about the shock (as is done in the present report), then the momentum is conserved across the shock, and the drag must then be identically zero. Care must be therefore exercised in the choice of the proper form of the conservation equations, since if the equations are used in the improper conservation form or in the non-conservation form such that the conservation of momentum is not preserved across the shock, then an erroneous pressure drag would result precisely equal to the erroneous decrement in the momentum conservation across the shock. In a numerical calculation truncation errors seldom permit the drag to vanish exactly; the finiteness of the drag would then be a measure of the accuracy of the calculations. If, however, the Von Karman-Guderley transonic small perturbation equations are used, again in such a way that the shock jump conditions in a consistently simplified form are fulfilled, one finds that an exact integration of the streamwise component of the surface pressures will not integrate to a zero drag. This apparent paradox results since the conservation of momentum across the shock is fulfilled only to within the small disturbance approximation, and the drag that is obtained would just match the decrement in momentum conservation due to the inadequacy of the simplified theory. (Provided of course the nose region is calculated properly, which is seldom accomplished.) Thus in a properly formulated isentropic theory the consideration of drag, in particular, drag divergence, is beyond the scope of the theory, while on the other hand, the determination of the pressure distribution, and hence lift and moment, is well within the prediction scope of the isentropic theory so long as the resulting shock strengths are no stronger than those experienced in experiments.

The above remarks apply of course only for $M_\infty < 1$. For $M_\infty = 1$ and $M_\infty > 1$ shock pressure drag can arise in an isentropic flow by the loss of streamwise momentum by radiation through "supersonic windows" that open up in the lateral far field.

3. FACTORS AFFECTING COMPUTER COSTS

Consideration of the computer costs in a finite difference analogue must already commence with the manner of formulation of the initial-boundary value problem on which the analogue is based. The equations should of course be used in the simplest form possible, both in terms of the complexity of the terms and their numbers as well as in the number of equations itself, weighed of course with the desired range of applicability of the resulting equations. Thus the simplest meaningful set of equations in the unsteady approach is the Guderley-Von Karman equations with fictitious time derivatives, Eqs. (21). These equations are in the proper conservation form conforming to the definition of Lax's weak solution. Here the assumption of small disturbances will impose limits on the class of profiles that can be treated. In the steady case with the small disturbance equations one has the choice of either having two first order equations in $\tilde{u}$ and $\tilde{v}$, or one second order equation in the perturbation potential. Here the reduction of the number of equations must be weighed against the increase in the order of the equation, as well as the increased accuracy with which the potential must be determined to obtain a given accuracy in its derivatives which are the physically meaningful quantities. Having to deal with one quantity, the potential, instead of the two velocities will, on the other hand, reduce the computer storage requirements. Simplest equations frequently arise when they are expressed in cartesian coordinates. Since the latter coordinate system invariably leads to a near-intolerable incompatibility with the boundaries on which conditions are prescribed, some compromise here must be sought, though generally the simplicity of the equations must be sacrificed at least locally.

Consider next the boundary conditions, in particular that at the airfoil surface which is probably the most crucial. With respect to the condition itself, it is invariably most preferable to prescribe an explicit non-homogeneous condition in terms of only one of the dependent variables; that is, it is more preferable to have a condition such as $v = h^{\pm}(x)$ at the airfoil surface, than $v = h^{\pm}u$, where $h^{\pm}$ is a known function. The "tieing down" of the value of one of the unknowns at the boundary here should in a numerical procedure which is marginally stable lead to greater stability than if the homogeneous condition were used. Where only the more exact homogeneous airfoil condition suffices, it will be more effective to set initially

$u = u_\infty$ (freestream value) to obtain initially an explicit non-homogeneous condition of the type $v = h^{\pm}(x)$, and then upgrade u by an iterative procedure. In imposing the condition it is most convenient to be able to impose it, not on the exact boundary, but on a neighboring boundary which is more compatible with the coordinate system, as in the case of the classical planar conditions. Where such planar conditions are inadequate, as we shall soon see is the case in the nose region of a blunt-nosed body, it may be sufficient to fulfill the exact conditions on a simplified neighboring non-planar boundary conforming exactly to the airfoil only where it is necessary. We shall illustrate one example of this in a later section. Another example where such a simplification might be used is in the procedures where the airfoil is mapped onto a circle. Here a simpler mapping might be considered, where only the nose region for example is mapped exactly onto the circle while the remainder of the profile is mapped to the neighborhood of the circle. The exact boundary condition would, of course, be prescribed on the circle in a "quasi-planar" way.

Let us turn next to the finite difference analogue for the unsteady case assuming here that we start with the simplest formulation of the problem suitably compromised to be consistent with our requirements. There are three factors that now determine the overall computer time. The first factor concerns the amount of calculation required for an elemental step where the solution at a given point is advanced to the next time step. Here an important consideration is the choice of the difference scheme. There are of course a multitude of difference schemes which have been suggested, but it will suffice here to discuss explicit schemes only, and among these only Lax's first order diffusing scheme (Ref. 4), and the two step Lax-Wendroff second order scheme described by Richtmyer (Ref. 13). There have been suggested other more elaborate schemes of second order accuracy which appear to be more effective under special conditions, but in general the added complexity beyond the straight-forward Lax-Wendroff scheme does not appear to be warranted. Quite obviously the second order Lax-Wendroff scheme for a given mesh spacing will yield a smaller truncation error in the marching process, and hence a more exact solution than a first order scheme, but of course at the expense of requiring more arithmetic steps. In the problem in the (x, y, t) system, in the second order scheme five first order schemes are in fact required. The mesh size required in the x, y, or t directions to obtain a given accuracy depends on the gradient of the dependent variables which arise in these directions. Assume that in a given case that the required mesh dimensions Δx and Δy are equal. The largest step Δt that is permitted for linear stability is dictated by the Courant, Friedrichs, and Lewy condition in the form, $\Delta t < \text{const.}\ \Delta x$, a statement requiring the point at the

new time to fall within the region of influence of the initial data. Thus in a hypothetical case assume that with the first order scheme half the mesh size Δx used for the second order scheme is required to obtain the same accuracy. This then means that 2^3 elemental calculations must be carried out with the first order difference scheme in contrast to one elemental step involving five first order differences for the second order scheme, a reduction of computer time by a factor 5/8 for the latter scheme. Unfortunately in a given unsteady planar flow problem the situation is not so clear cut, with the precise merits of the first and second order schemes for a sufficiently small spacial mesh being determined largely by the time rate of change of the developing flow. Quite clearly if the flow is only changing slowly with time, the first order scheme may be entirely adequate, while on the other hand the first order scheme will be entirely inadequate when the flow has experienced a large unsteadiness prior to its approach to the steady state. In the latter situation the first order scheme is quite adequate to handle the slowly changing approach to the steady state, but it has suffered a large truncation error during the unsteady phase from which it can never recover, resulting in an erroneous steady asymptotic flow. The latter behavior has been found in several calculated examples involving a blunt-nosed supercritical profile. In fact for these test cases the first order scheme was found to be entirely inadequate, and only the use of the second order scheme led to viable results. Quite obviously an attractive procedure suggested here is the use of the second order scheme to treat the more unsteady phase of the time history, and then switch to the first order scheme in the slow approach phase to the steady state.

In passing it may be noted that the use of the two step second order Lax-Wendroff difference scheme in the unsteady planar equations in conservation form leads to a "telescoping" feature leading to the automatic fulfillment of the integrated conservation laws. (See Richtmyer, Ref. 13).

The second factor influencing the computer time is the total number of mesh points which are required ultimately in the x, y plane to describe the final steady flow. The mesh spacing here is simply dictated by the flow gradients. Quite obviously economy would suggest the use of a variable mesh spacing to fit the final velocity gradients, but this cannot be overdone since a wasteful overlap of the different sub-domains with a given mesh must be provided to assure continuity of the flow. In the early efforts it was thought that the initial phases of the developing flow could be treated by a coarse spacial mesh to establish the intermediate and far field flows rapidly, and only after this introduce a refinement of the mesh about the airfoil to recover a viable near field flow. This simply did not work out, at least for blunt nosed supercritical profiles, since the strength of the "singularities"

to be communicated to the intermediate and far fields were never adequately developed in the near field, due to the coarse mesh, in particular, the contribution of the nose flow. Another means to decrease the number of mesh points is simply to redefine the dependent variables such that the sought quantities at the new time are differences from the initial values. Such differences will have significantly decreased gradients, especially in the long duration approach to the steady state, so that the spacial mesh size can be accordingly increased. Since as we have seen earlier, the computing time varies inversely as the cube of the mesh dimension, such a simple change of dependent variable should have a dramatic impact especially in the vicinity of a highly blunt nose where generally an early attainment of steady conditions results and where a disproportionate number of mesh points is required. In this change of variables, most probably a linearization can be justified except perhaps about the shock if the shock location is changing. In a version suggested in Ref. 14 to be studied shortly, the non-linearity was retained. Here it is important to reexamine the impact on the shock jump conditions.

Finally the third factor affecting computer costs is the rapidity with which the desired steady state is obtained. The last procedure described above will clearly have a bearing here also. Another important facet here is the choice of the initial data itself. Quite clearly the proximity of the initial flow to the final flow is of significance, but the route between the two is not always direct as was found in several calculated examples, where a slowly oscillating apparently near-undamped shock sequence was obtained. The simple cure here is simply not to prescribe an initial flow which is susceptible to this phenomenon (though we do not of course have a clear cut criterion for this) by using "adjusted" initial data which places the shock somewhat upstream of the expected location to provide a fast adjustment path for the flow to adjust to the desired state.

In summary the path suggested to reduce computer time without sacrifice of the accuracy of the solution is to tailor not only the formulation of the problem but also its analogue, both in space and time, to be "just adequate." Thus in regions not containing a shock the equations in the simpler non-conservation form is suggested, while about the shock the appropriate conservation forms must be used. At a blunt nose the exact boundary condition should be applied at the exact surface while elsewhere the condition may be fulfilled in a quasi-planar way on a simpler boundary in the neighborhood of the airfoil surface. In the analogue a variable spacial mesh spacing to fit the anticipated flow gradients should be used; the two step second order Lax-Wendroff difference scheme must be used during the initial unsteady phase

converting to a first order scheme with a change of the dependent variables without a linearization in the final time consuming approach to the steady state. Quite obviously the extent to which the above philosophy should be implemented must be weighed against the increased program logic and storage required as well as by the wasteful overlap and added complications to avoid a mismatch at boundaries where the procedures are patched.

In the next section we shall first examine whether the Guderley-Von Karman equations with fictitious time derivatives and with planar boundary conditions are adequate to treat blunted nosed supercritical profiles. This is then followed by a more exact formulation incorporating some of the suggestions given above.

4. INVESTIGATION OF THE SIMPLIFIED PROBLEM

In the present section we shall first describe the finite difference results using the Guderley-Von Karman small disturbance equations as given in Eq. (21) with a planar boundary condition at the airfoil. The test case will be the flow at $M_\infty = 0.80$ over the supercritical profile of 11% thickness ratio at $\alpha = 0$ calculated earlier in Ref. 3 with the exact conservation equations (23). This case was selected because

a. It is fairly representative of the current problems on which one might want to employ the numerical analysis.

b. The moderately large thickness (11%), heavy cambering, considerable nose blunting (2.2%) and fairly high local Mach numbers would provide severe tests of the ability of the simplified equations and boundary conditions to describe adequately the flow.

c. A solution obtained by the numerical method described in Ref. 3 was available for comparison.

In the calculations a modification of Richtmyer's two step version of the second order Lax-Wendroff difference scheme has been used with an inclusion of some diffusive damping. (See Ref. 2). As is well known this explicit difference scheme is stable only if the marching increment Δt is kept below some limiting value dependent on local conditions. For simplicity the allowable Δt has been determined for a representative range of u and v to be encountered in typical airfoil problems. The complex amplification of small disturbances of various wave lengths and orientations was determined as a function of the marching increment, Δt, and limiting values which would keep

the absolute value of the amplification below unity were chosen. These limits were then examined as functions of u and v, and an overall limit, $\Delta t \leq 0.15\ \Delta x$ was chosen. This limit is highly conservative around the stagnation point and is closest to the actual stability limit for sonic flow at an inclination near 30° to the x direction.

The preceding remarks on stability and damping apply to the centered difference schemes used at ordinary field points. At the airfoil surface (or, rather, the chordline slit) where boundary conditions are to be imposed, compatible non-centered difference schemes were devised. That is to say, special schemes were constructed to have the same nominal order of accuracy as the ordinary schemes. These were also screened by checking amplification of small disturbances of various wave lengths and orientation. This screening was considered necessary but insufficient to prove stability inasmuch as the presence of the boundary can shift disturbance energy into disturbances of different wave length and orientation; this would be incompatible with the fundamental assumptions in the linearized stability analysis which is being employed. The boundary schemes are of the Lax-Wendroff one-step class with special matrices for the stabilization terms. The orientation of the boundary with respect to the mesh influences the magnitudes of the elements of the stabilization matrices.

In the calculations a cartesian mesh system was employed about the airfoil overlapping with a polar mesh system in the far field. Approximately 3500 mesh points were typically used distributed as shown in Table 1. Here the airfoil chord is of unit length with the nose located at the origin.

In the present problem the flow about the leading edge is singular. To avoid this region in the calculation, a similarity solution for a parabolic nose at zero incidence is used in a 0.0125 chord square domain centered about the slit terminus. This similarity solution is defined in terms of the perturbation potential by the hypothesis

$$\varphi = |\eta|^{4/7} F(\zeta)$$

where

$$\zeta = (\gamma + 1)^{-1/3} \xi |\eta|^{-6/7}, \text{ and}$$

$$(36\zeta^2 - 49F')\, F'' + 30\zeta F' - 12F = 0 .$$

Table 1. Typical Mesh Arrangement

Region	$\Delta x = \Delta y$	Range
Inner Nose Region	0.00625	$-.075 \leq x \leq .075$ $-.10 \leq y \leq .10$
Outer Nose Region	0.0125	$-.15 \leq x \leq .15$ $-.20 \leq y \leq .20$
Airfoil Region	0.05	$-.40 \leq y \leq .60$
Fine Outer Region	0.10	$-.70 \leq x \leq 1.70$ $-.80 \leq y \leq 1.20$
Coarse Outer Region	0.20	$-1.10 \leq x \leq 2.10$
Outer Polar Region	$\Delta r \geq 0.2$ $\Delta\theta = 9^{\circ}$	$1.4 \leq r < \infty$ $-9^{\circ} \leq \theta \leq 360^{\circ}$

In Fig. 1 we now show the resulting surface pressure distribution in terms of the pressure coefficient C_p given in accordance to small disturbance theory as

$$C_p \equiv \frac{p - p^*}{q^*} = -2\tilde{u} .$$

Here for comparison is shown the results from the more exact calculations from Ref. 3. The comparison shows a drastic discrepancy in the nose region, both on the upper and lower surfaces, with the simplified solution exhibiting a horrendous nose over-expansion. There is further a discrepancy in the shock location and in the over pressures on the lower aft surface. In the plateau region, on both the upper and lower surfaces, there is good agreement. It is thus amply clear that the small disturbance simplifications are inadequate at least for the test example.

The cause of the above discrepancies can be attributed to the combination of the inadequate equations, and an inadequate airfoil boundary condition imposed at an inappropriate boundary. To separate these effects we have next calculated for the same test flow the following four additional cases characterizing each case in the following by noting the equations and the airfoil boundary condition used.

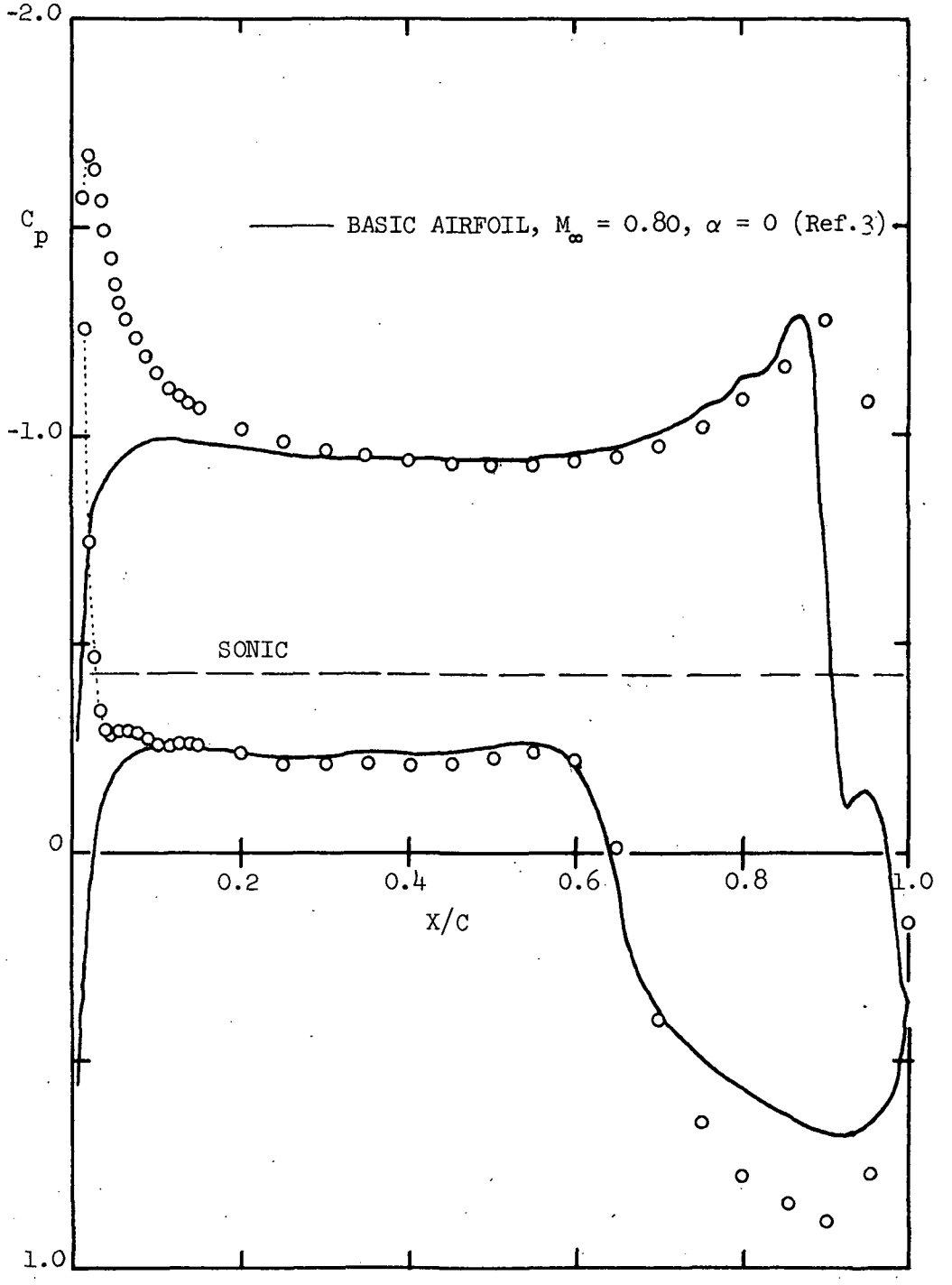

Figure 1. Results of the Guderley-Von Karman Small Distribution Problem

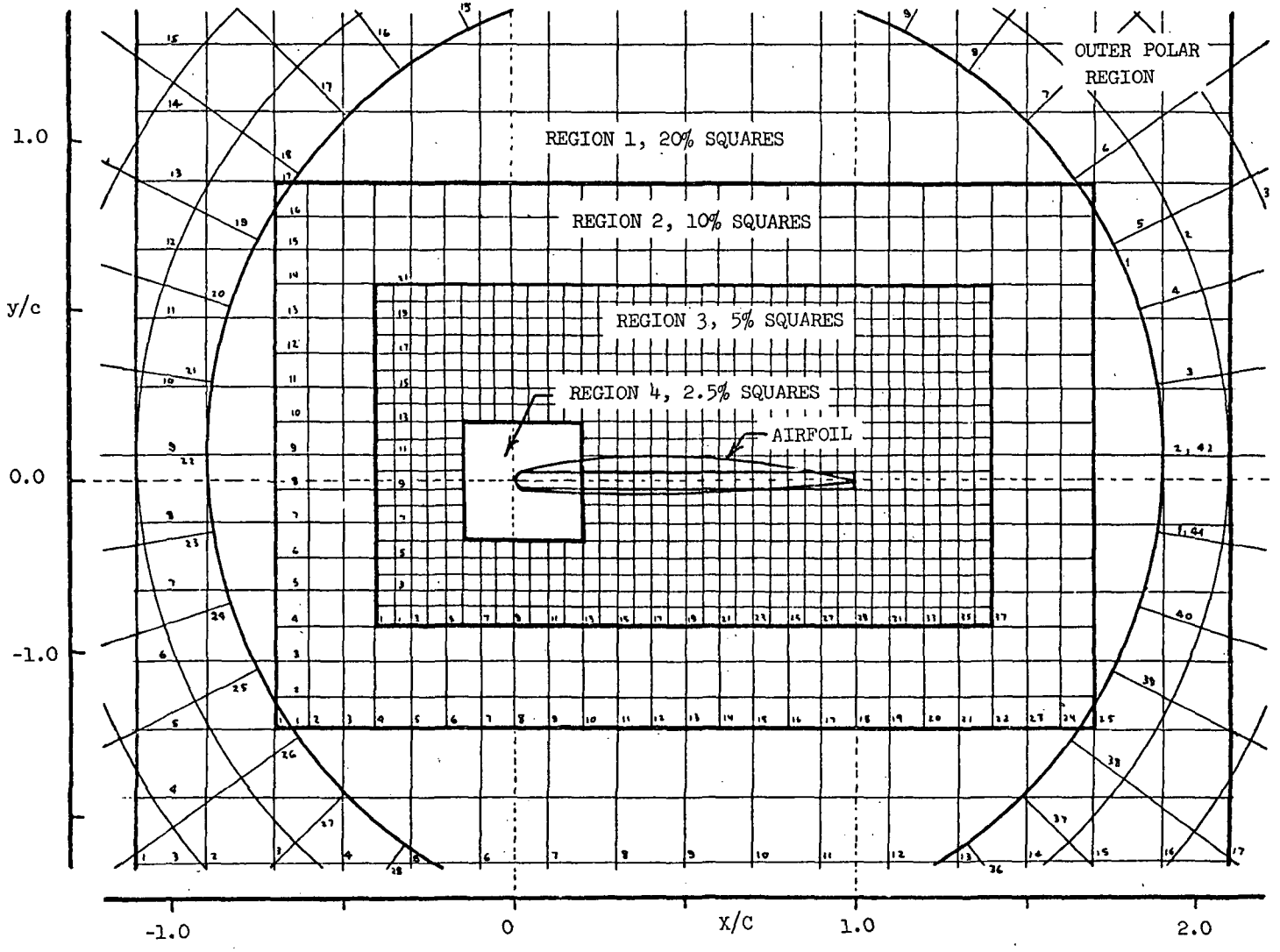

Figure 2(a). Mesh Arrangement for Calculations Based on Blunted Slab

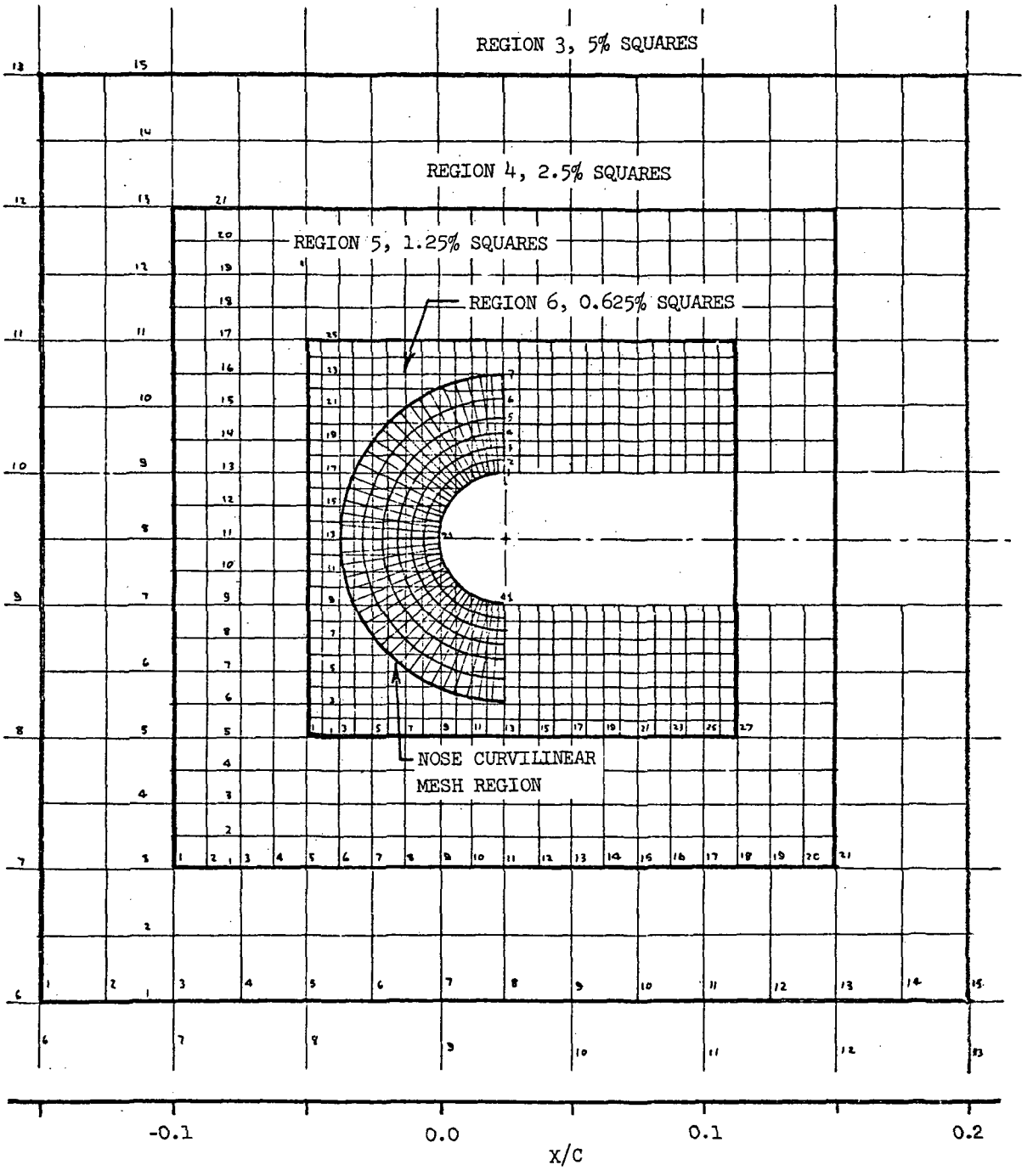

Figure 2(b). Mesh Arrangement for Calculations Based on Blunted Slab

I. Equations: Exact non-conservation form - Eq. (22).
B.C.: Planar condition.

II. Equations: Small disturbance.
B.C.: Exact condition [$\tilde{v} = (1 + \tilde{u}) \tan \theta$] fulfilled on a slab described earlier in a first order planar fashion.

III. Equations: Exact in non-conservation form.
B.C.: Exact (Same as II).

IV. Equations: Exact in non-conservation form.
B.C.: Exact condition fulfilled on slab in second order.

For the cases where the airfoil condition is fulfilled on the slab, the mesh configuration is shown in Figure 2 and detailed in Table 2. The resulting surface pressure distribution for these cases are shown in Figs. 3-6. Consider first Fig. 3 (Case I) with the exact equations with planar conditions. It is seen here that the nose overexpansions have been somewhat subdued on the upper surface by the more exact equations, but have been "over-subdued" on the lower surface to the extent that the plateau pressures have been additionally distorted. Planar conditions are clearly inadequate in the nose region. The previous discrepancy in the overpressures on the lower aft surface has been remedied by the more exact equations, so that planar conditions appear to be adequate except for the nose region. The shock wave is still inadequately treated, but this is most probably the consequence of not using the equations in conservation form.

The results of Fig. 4 (Case II) with the approximate equations and the exact boundary condition illustrate the importance of having the proper condition at the nose. The discrepancy due to the inadequate equations at the nose now appear to be reduced to the order of that along the aft portions of the airfoil. Fig. 5 (Case III) shows that the use of the exact equations in non-conservation form and the exact slab boundary conditions gives reasonable agreement with the reference calculations except at the nose where a slightly increased loading arises, and at the shock. In Case IV an improvement of Case III is sought by simulating the fulfillment of the boundary condition at the actual airfoil surface by imposing a modified condition on the slab (second order planar condition) which assumes the velocities u and v to vary linearly from the actual airfoil surface to the slab. The results for Case IV in Fig. 6 show some improvement due to the improved boundary condition, but there still remains a small discrepancy on the lower surface.

Table 2. Mesh Arrangement, Blunted Slab Approximations

Region		Range
Cartesian 1	$\Delta x = \Delta y = 0.2$	$-1.1 \leq x \leq 2.1$ $-1.525 \leq y \leq 1.675$
Cartesian 2	$\Delta x = \Delta y = 0.1$	$-0.7 \leq x \leq 1.7$ $-0.725 \leq y \leq 0.875$
Cartesian 3	$\Delta x = \Delta y = 0.05$	$-0.4 \leq x \leq 1.4$ $-0.425 \leq y \leq 0.575$
Cartesian 4	$\Delta x = \Delta y = 0.025$	$-0.15 \leq x \leq 0.2$ $-0.175 \leq y \leq 0.175$
Cartesian 5	$\Delta x = \Delta y = 0.0125$	$-0.1 \leq x \leq 0.15$ $-0.125 \leq y \leq 0.125$
Cartesian 6	$\Delta x = \Delta y = 0.00625$	$-0.05 \leq x \leq 0.1125$ $-0.075 \leq y \leq 0.075$
Curvilinear Nose	$\Delta\theta = 4.5^{\circ}$ $0.0040 \leq \Delta r$	$90^{\circ} \leq \theta \leq 270^{\circ}$ $0.025 \leq r \leq 0.0625$
Outer Polar	$\Delta r \geq 0.2$ $\Delta\theta = 9^{\circ}$	$1.4 \leq r < \infty$ $-9^{\circ} \leq \theta \leq 360^{\circ}$

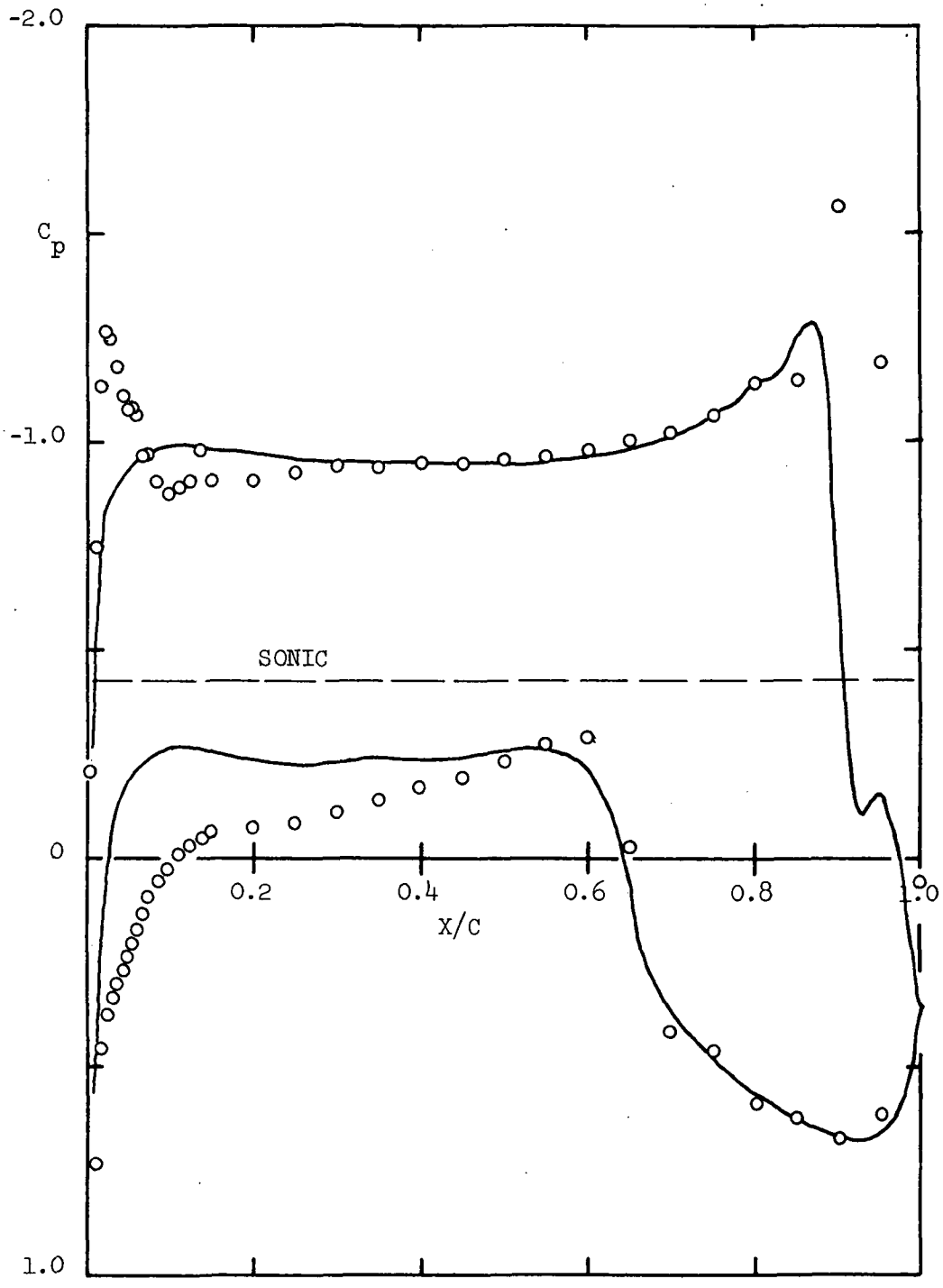

Figure 3. Results for Case I - Exact Equations and Planar Conditions

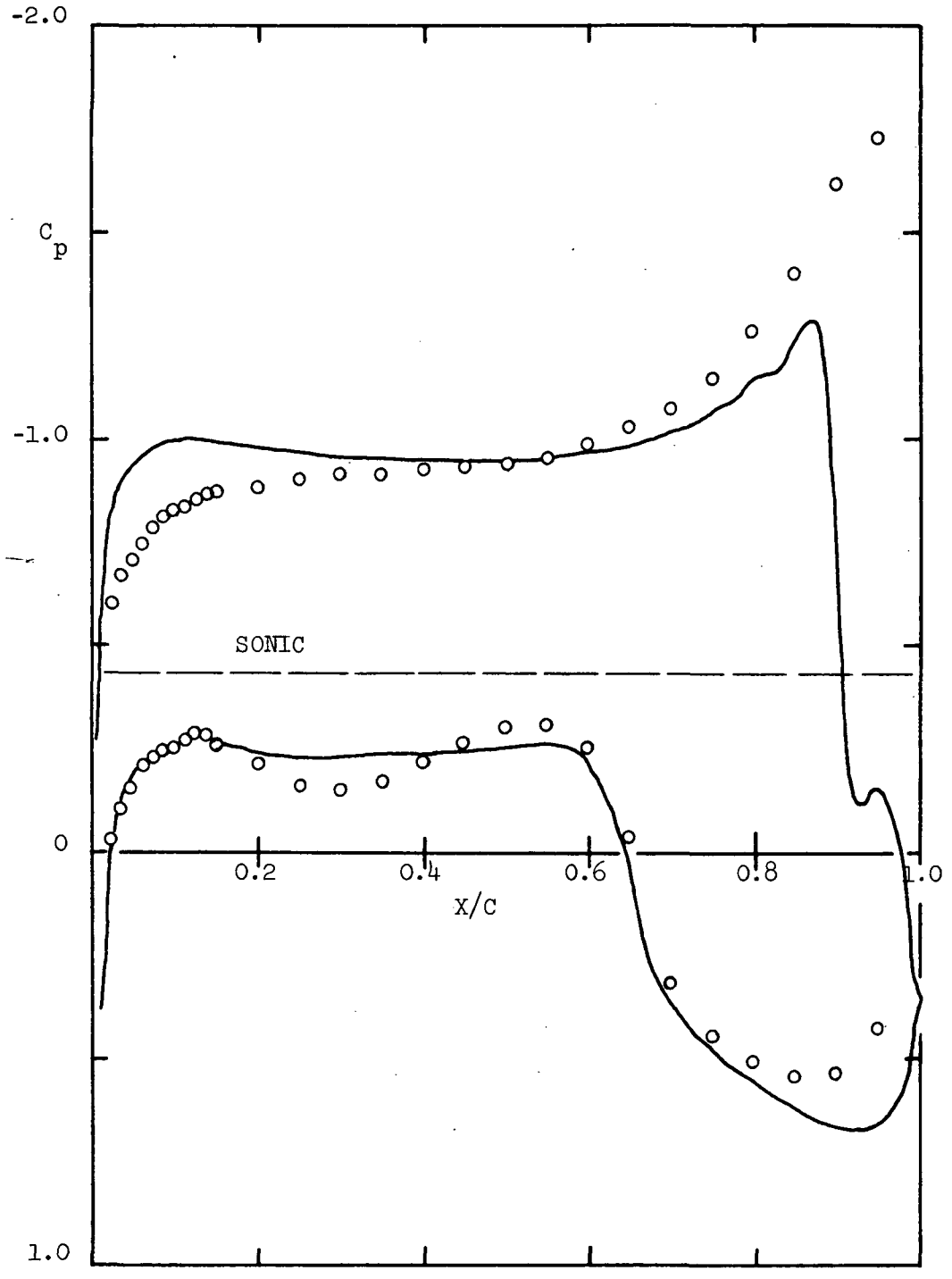

Figure 4. Results for Case II - Small Disturbance Equations and Exact (First Order) Slab Conditions

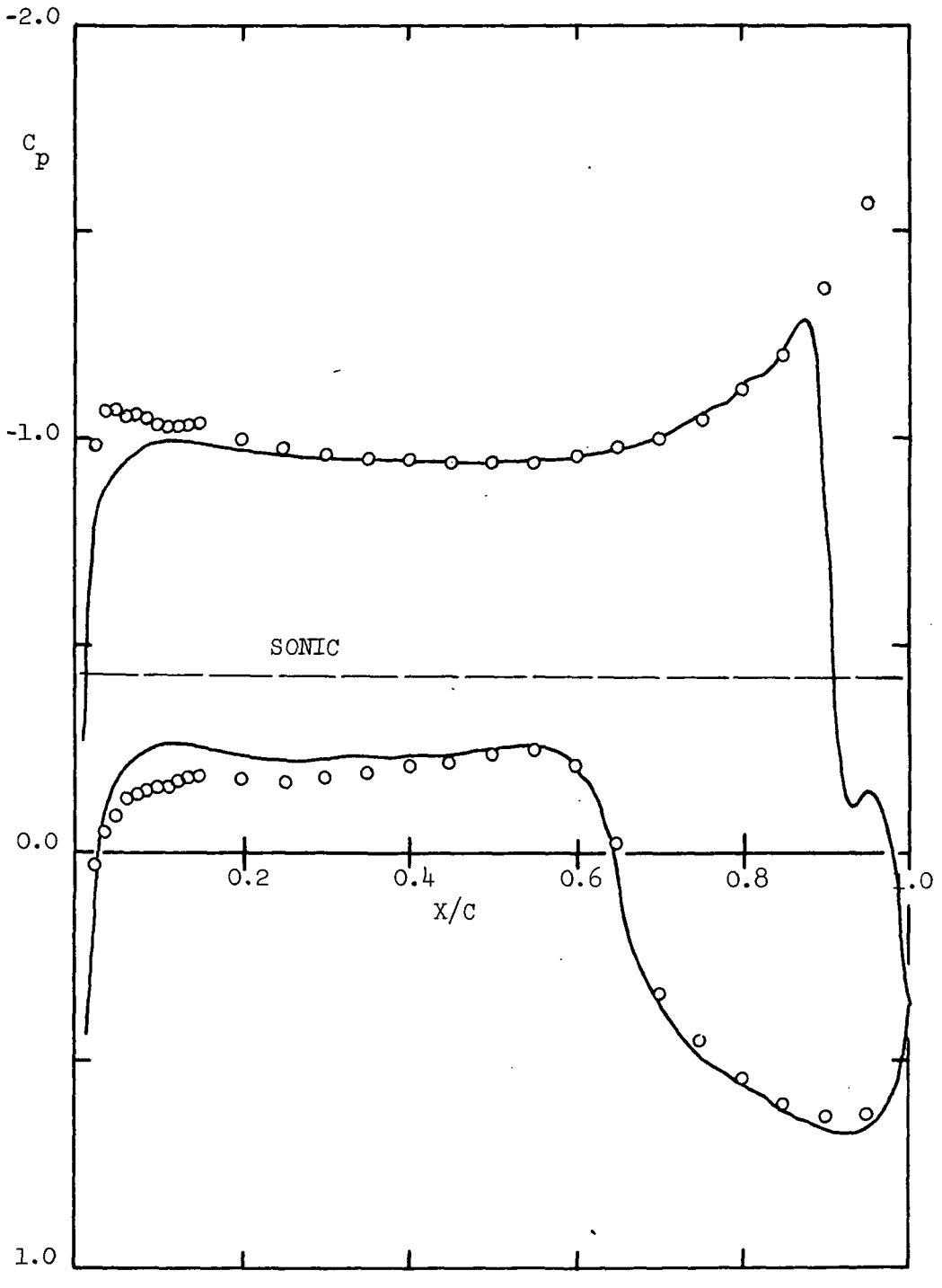

Figure 5. *Results for Case III - Exact Equations and Exact Slab (First Order) Condition*

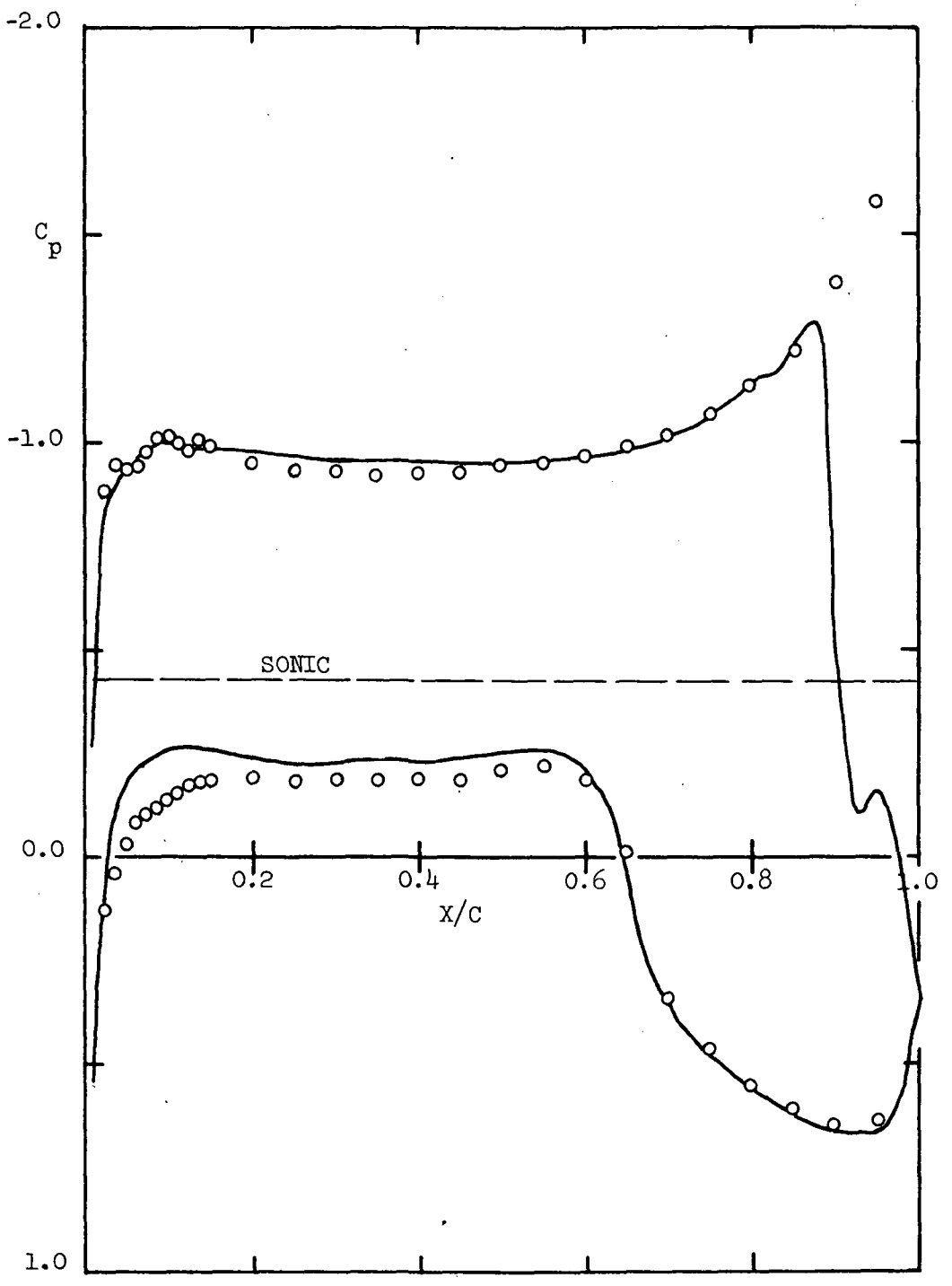

Figure 6. Results for Case IV - Exact Equations and Exact (Second Order) Slab Conditions

Thus in summary we note the following:

b. The exact condition must be prescribed at the actual airfoil surface in the nose region, while it may be prescribed in a quasi-planar manner over the remainder of the profile. The slab condition should thus be adequate.

b. The exact equations must be used, and they probably must be used in conservation form about the shock. (We shall check the latter in the next section.)

It must be remembered that these conclusions pertain to the more "severe" profiles and flow conditions, and that the Guderley-Von Karman formulation of the problem is most certainly adequate for a wide class of other less severe airfoils and flow conditions.

5. PROCEDURE WITH THE PROPER EMBEDDED CONSERVATION EQUATIONS

In the unsteady procedure for further consideration, the equations with the exact steady terms in u and v with fictitious time derivatives as given in Eq. (22) will be used in the continuous regions of the flow; and the exact unsteady Euler equations in ρ, u, and v in the proper conservation form as given in Eq. (23) will be used in the subdomain embedding the shock. There is then an incompatibility of the time derivatives which would vanish as the steady state is attained. The exact boundary condition, as previously, will be fulfilled on the slab. In the subdomain embedding the shock a fine mesh of 1.25% chord will be employed.

With the above system of equations several examples have been calculated. Two of the examples were calculated earlier with the original unsteady procedure of Refs. 2 and 3, and they will serve as check cases for the revised procedure. Additionally in the present calculations reduced diffusive damping will be employed to capture the shocks more exactly.

The first example calculated is the 11% aft-cambered profile at $M_\infty = 0.8$ and $\alpha = 0$ which was computed earlier in Ref. 3 (see also Ref. 8). The resulting surface pressure distribution is compared with the earlier result in Fig. 7. Here the agreement is reasonably good over most of the airfoil, but there still remains the discrepancy in the nose pressures observed earlier, and the shock has now been displaced essentially to the trailing edge, where an insufficient flow resolution with the mesh used precludes its proper capture. The obvious suspect causing these discrepancies is the application of the

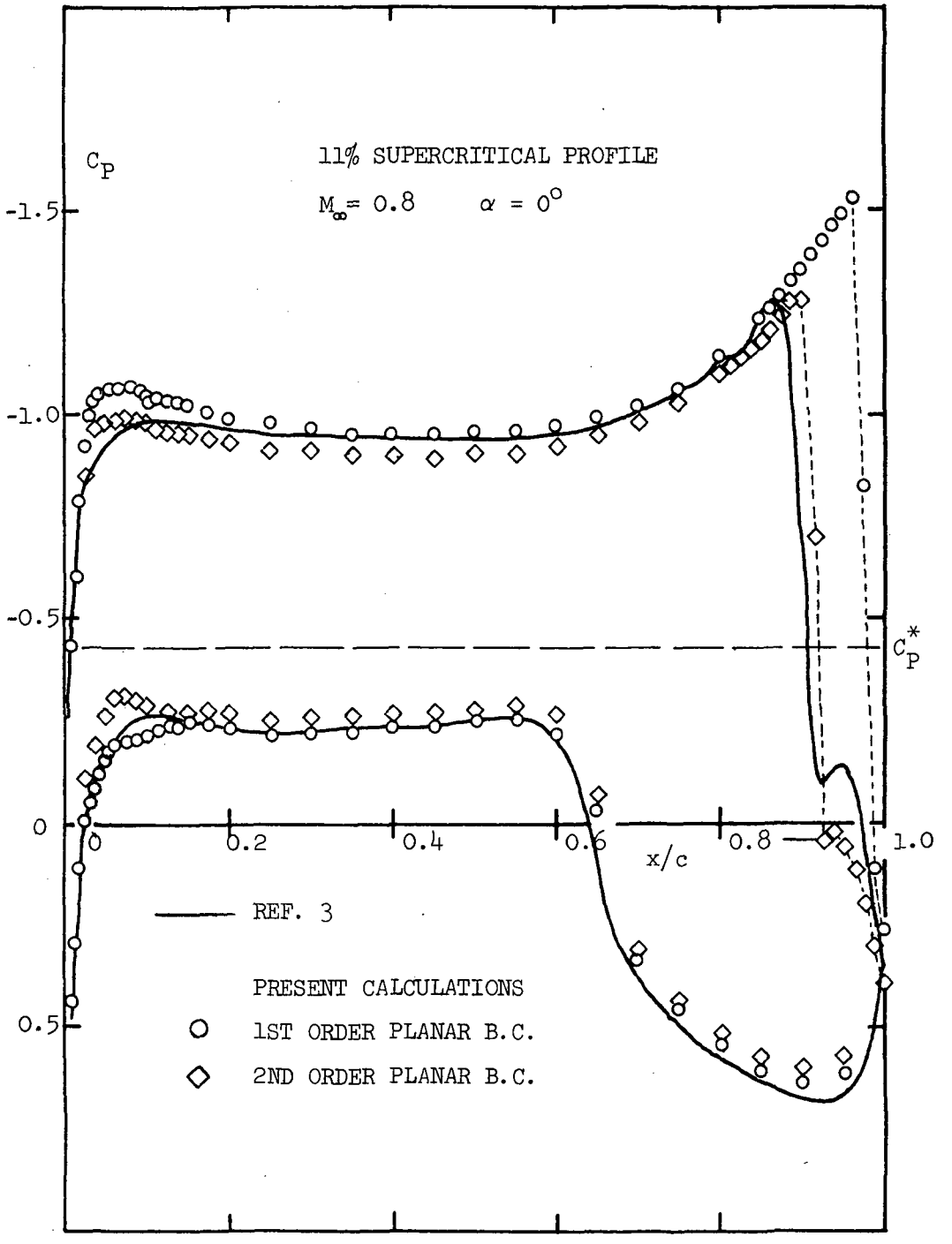

Figure 7. Comparison of the Pressure Distributions Calculated by the Unsteady Procedures.

airfoil boundary and Kutta conditions on the slab rather than on the actual airfoil. To check first the extent that the streamline slopes θ differ at corresponding points on the slab and the airfoil, we have shown in Sketch D the lines of constant θ (isoclines) from the earlier calculation about the aft portion of the profile where the largest differences can be expected. It is of interest here to note first the differences of the isocline patterns in the different subdomains, but only in the subsonic region aft of the shock are the isoclines such that a significant difference arises in the θ distributions along the slab and the airfoil surface. In the present calculations we have prescribed the actual airfoil slopes along the slab, whereas Sketch D would indicate that less inclined slopes should have been prescribed. The present results with the slab would thus represent the flow for a profile with a somewhat greater aft camber than desired, and this difference could readily explain the greater expansion at the nose and the more downstream location of the shock. To verify this we have repeated the calculations using a more exact planar condition applied on the slab which takes into account the variation of θ between the slab and the airfoil. The second order planar condition used assumes a linear variation of θ with y in this neighborhood where the gradients θ_y are taken as the values obtained in the calculation at the slab. The resulting pressure distribution is shown in Fig. 7. The shock here has now been displaced upstream of the trailing edge and has been properly captured, but there now arises a small discrepancy in the plateau pressures on both the upper and lower surfaces indicative of insufficient aft camber. The probable cause of this deficient aft camber effect is the inadequacy of applying the Kutta condition on the slab. Examination of the earlier more exact results, where the boundary and Kutta conditions were imposed on the airfoil, shows that the pressures at the points on the slab corresponding to the trailing edge are not equal, but in fact a small difference arises characteristic of a case with a jet flap. Thus to regain the proper plateau pressures one must now permit a small jump in the trailing edge pressures on the slab, where the jump can be ascertained in the same manner as the slopes θ were previously corrected. In the calculations where the first order planar slab conditions were used, as noted earlier the plateau pressures agreed closely with the earlier exact case, but in light of the above discussion this close agreement is somewhat fortuitous since the effects of the deficient first order planar condition apparently were just compensated for by the missing jet flap effect. Thus for extreme profiles as the present one, it is essential to apply on the slab the second order corrections to the slopes, while less important, a correction should also be considered for the trailing edge pressures.

The second example calculated is that for the NACA 64A 410 profile at $M_\infty = 0.72$ and $\alpha = 4^\circ$. The results of the present calculation are compared in Fig. 8 with a number of previously calculated pressure distributions from several methods as well as with the experimental results of Stivers. Directly comparable here are the present results, the result from Ref. 2, and the results

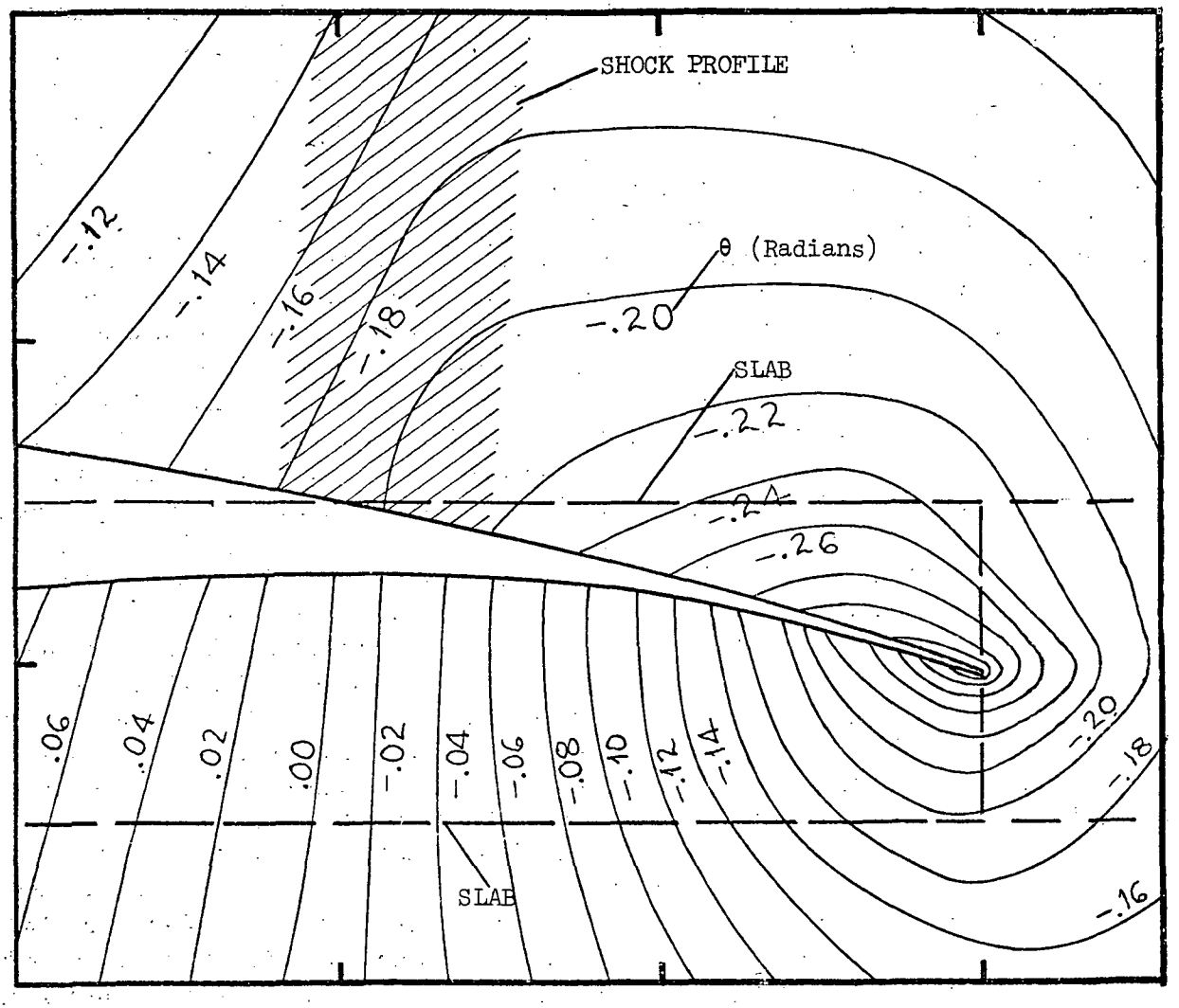

Sketch D. Isoclines for the 11% Supercritical Profile (Ref. 3).

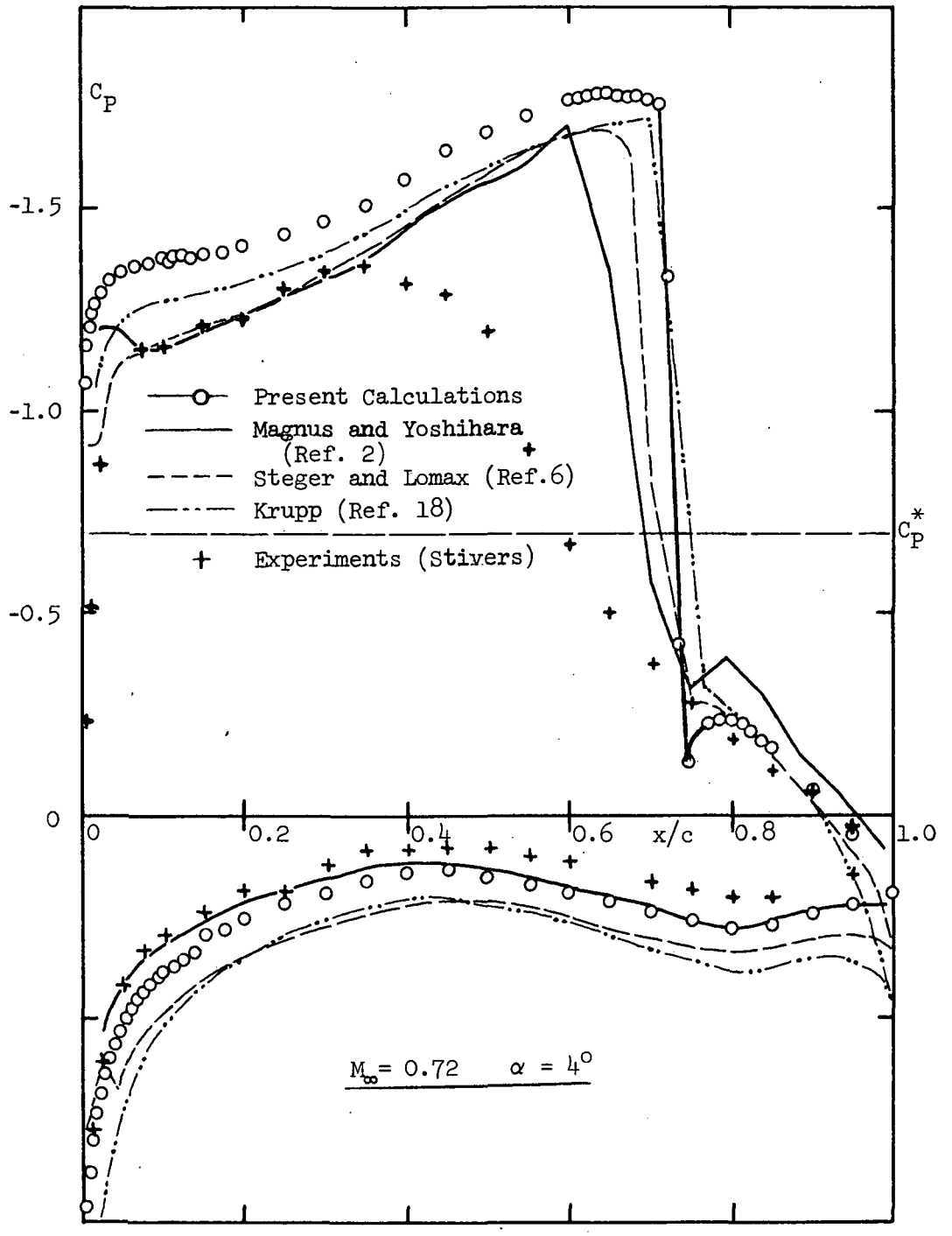

Figure 8. Comparison of Various Finite Difference Results for the NACA 64A-410 Profile.

of Steger and Lomax (Ref. 6). Consider first the comparison of the results from the unsteady procedures. The agreement of the pressure distributions over the lower surface is good, but there is a puzzling not insignificant discrepancy in the upper surface pressures ahead of the shock, most probably attributable to a discrepancy in the nose expansions. To check whether the use of the slab might account for a difference in the nose expansion, the fulfillment of the surface tangency condition at the actual airfoil nose was checked in the present results. In this highly inclined segment of the airfoil the resulting slopes at the actual airfoil surface were found to agree with the actual slopes to within less than a tenth of a degree, so that the use of the slab most probably must be ruled out as the source of the upper surface discrepancy. A comparison of the isobar distributions in the region about the nose however showed a significant difference. Whereas in the present calculation, where a more natural polar mesh system is used, the isobar pattern is smooth and near circular in shape, the isobars in the earlier calculation with a cartesian mesh system exhibited some irregularities (see Fig. 5, Ref. 2), and they were less reasonably shaped in general. One must therefore tentatively conclude that the difference of the mesh configurations about the nose and the patching of the various regions of different mesh sizes most probably were the causes of the difference in the nose expansions. The results of the present calculations, despite the fact that they now depart from Stiver's experimental results on the upper surface should supersede the earlier results. (Note that the early experimental results of Stivers, obtained in a closed tunnel at a low Reynolds number without a boundary layer trip, may be afflicted with wall interference effects as well as more importantly, viscous effects which may cause the lowering of the upper surface suctions ahead of the shock through a highly probable leading edge separation bubble). The use of the first order planar slab condition here will of course affect the upper surface pressure plateau, but the consequence should be relatively insignificant since the gradients of the streamline slopes are negligible about the aft portion of the upper surface. The present result further exhibits the proper jump condition, and there is sufficient resolution to yield a post-shock cusped pressure bucket. The improvement in the fulfillment of the jump conditions is also shown in Fig. 15. The present results for the NACA 64A 410 profile is also directly comparable with the results of Steger and Lomax shown in Fig. 8 where also the full steady Euler equations were used. The discrepancy between these results on both the upper and lower surface apart from the shock location and pressure rise, appears to be due to a difference in circulation brought about by the difference in the manner of imposing the Kutta condition.

The third example is also for the flow over the NACA 64A-410 profile but at $M_\infty = 0.735$ and $\alpha = 1^\circ$. In Fig. 9 we show the resulting surface pressure dis-

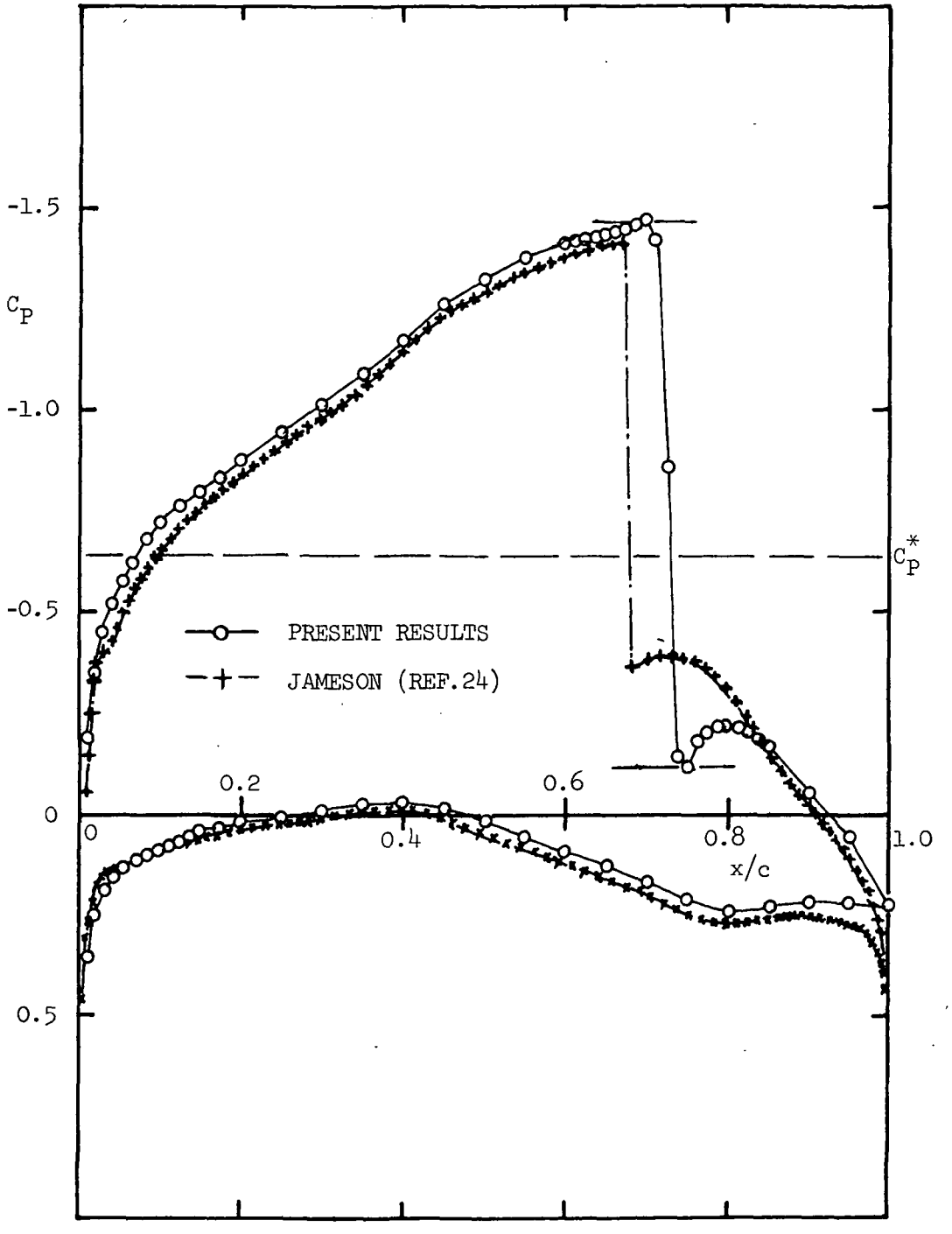

Figure 9. Pressure Distribution for the NACA 64A-410 Profile at $M_\infty = 0.735$ and $\alpha = 1^\circ$.

tribution where a comparison is also made with the results obtained by Jameson (Ref. 24) who used a steady relaxation procedure similar to that of Korn and Garabedian. The major discrepancy here in the two results is in the fulfillment of the shock jump condition and in the pressures just downstream of the shock. The desired condition downstream of the shock is indicated here by the dashed horizontal line, and it is seen that despite the fine mesh used, the result of Jameson does not capture the shock correctly. We shall discuss the treatment of shocks by the various steady relaxation procedures further in the next section.

The fourth example is an aft cambered profile of 3.9% thickness ratio at $M_\infty = 0.90$ and $\alpha = 0$. The resulting surface pressure distribution is shown in Fig. 10. Here only the first order planar slab condition was used, so that, as in the first example, when a second order planar condition is employed, one can expect a somewhat further upstream displacement of the shock.

The shock capturing ability of the present procedure is further examined for an aft-cambered airfoil (Airfoil A) previously calculated and tested at high Reynolds number (30×10^6/15 inch chord) at NAE (Ottawa) (See Ref. 15). The earlier comparison of the experimental and calculated result at $M_\infty = 0.85$ showed a remarkable agreement in the pressure distributions (see Fig. 11) everywhere except for the pressure along the aft portion of the lower surface, the location of the shock wave, and the pressures downstream of the shock, which understandably are the expected departures due to viscous effects. In the above comparison the angle of attack in the calculations was simply adjusted until the plateau pressures on both the upper and lower surface matched. Such a procedure could then be used to obtain an indication of the incidence correction due to wall effects for a highly porous perforated tunnel, if the viscous effects on the airfoil were negligible. Viscous effects, however, are not negligible for the aft-cambered peaky Airfoil A even at the high Reynolds numbers of 30×10^6/chord. Leading edge separation and the change of the effective aft camber due to the not insignificant boundary layer displacement effects on the aft portions of both the upper and lower surfaces will significantly alter the plateau pressure levels. It is somewhat fortuitous that a simple angle of attack correction under such a circumstance enabled one to obtain the agreement shown in Fig. 10. With the present updated unsteady procedure a further calculation was carried out as the fifth example in which a preliminary attempt was made to determine how the upper aft portion of the airfoil (the viscous ramp of Ref. 20) must be modified to move the shock to the experimentally observed location and to obtain the empirically measured pressures aft of the shock. The procedure was modified such that the experimentally measured pressures aft of the shock

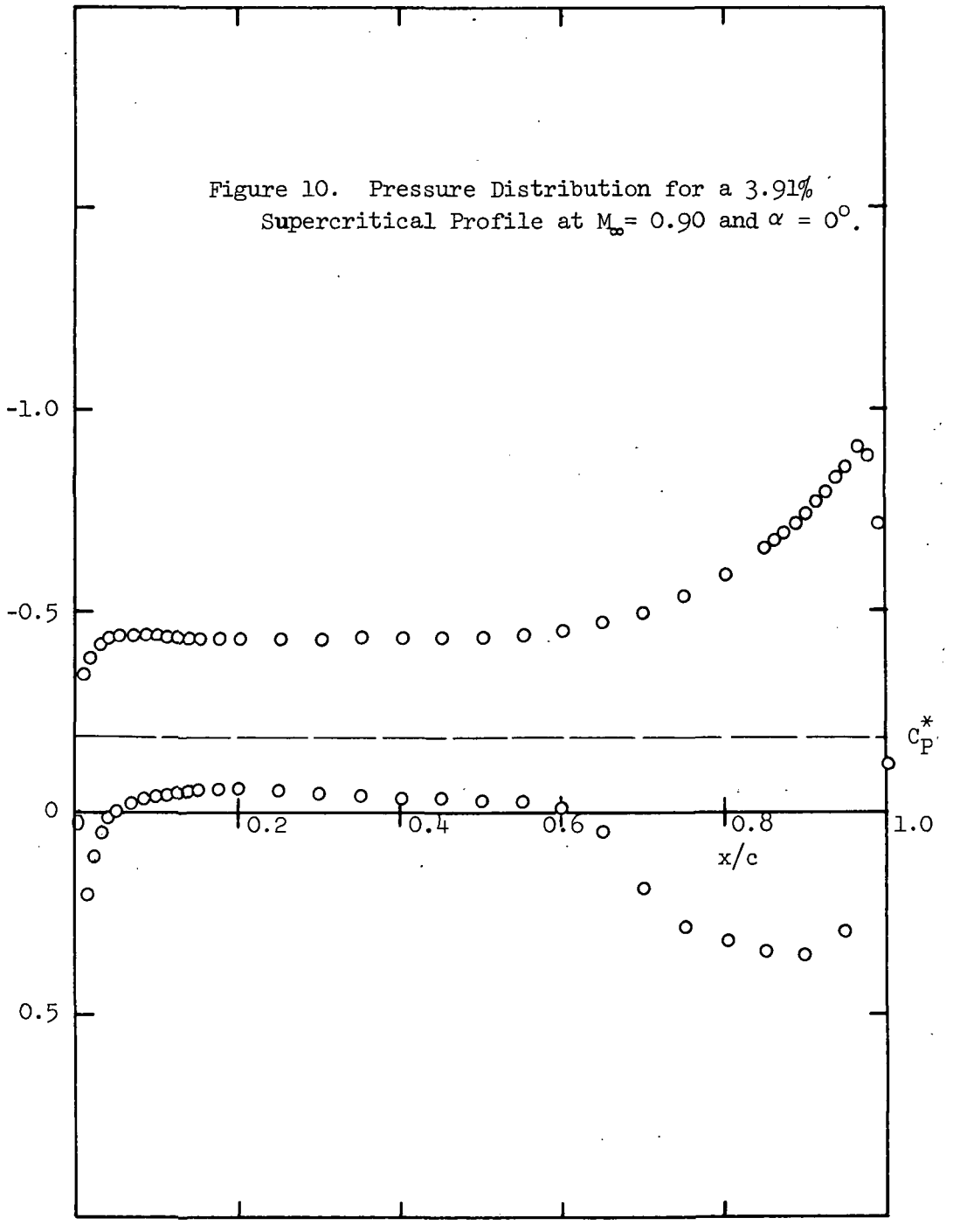

Figure 10. Pressure Distribution for a 3.91% Supercritical Profile at $M_\infty = 0.90$ and $\alpha = 0^\circ$.

AIRFOIL A

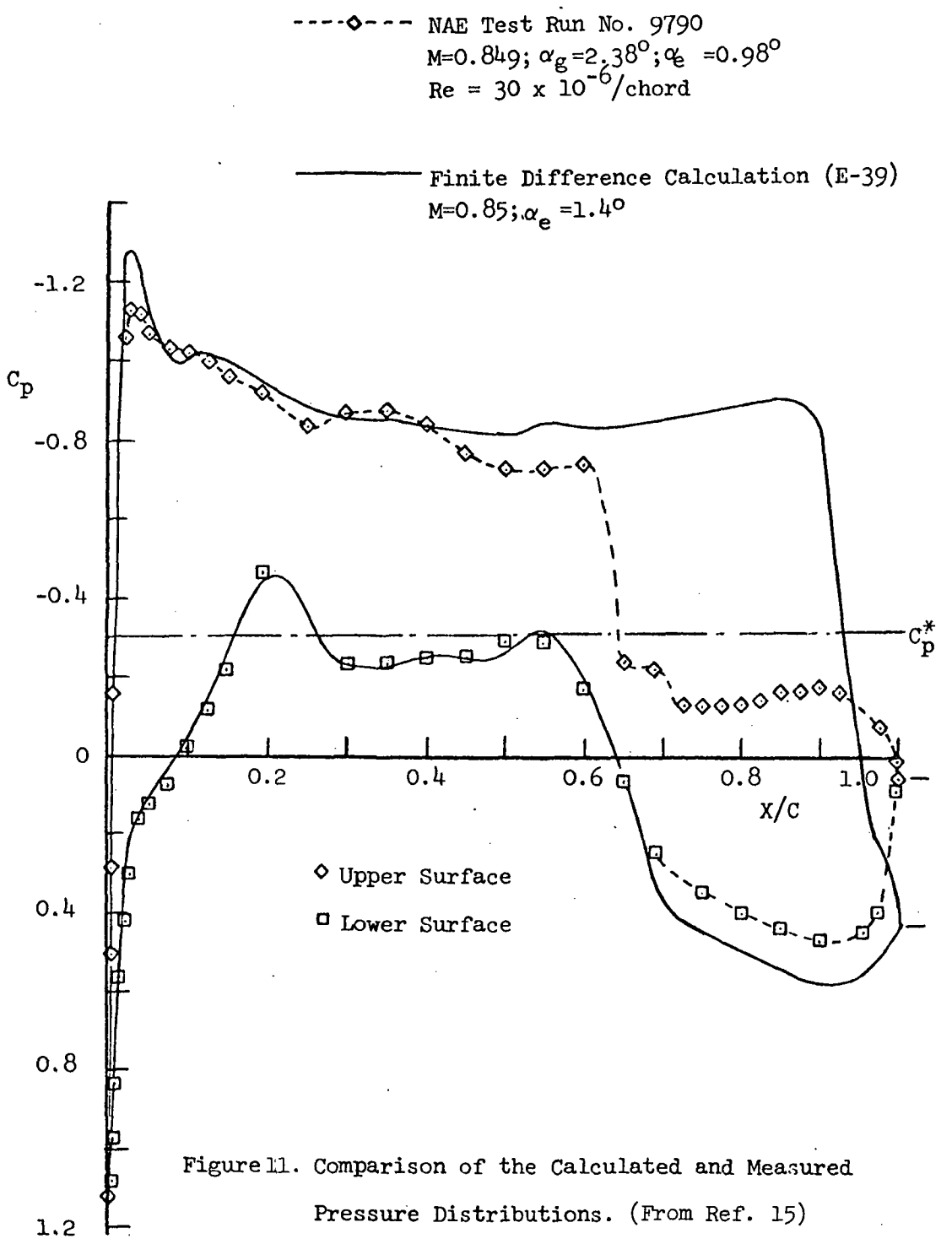

Figure 11. Comparison of the Calculated and Measured Pressure Distributions. (From Ref. 15)

on the upper surface could be prescribed, replacing the prescription of the airfoil shape. The results of the calculations would then yield the surface pressures where the shape was prescribed and the effective shape of the airfoil where the pressures were prescribed. Such a result could then be used to obtain the upper surface boundary layer displacement. In the initial calculation the angle of attack was taken at 1.4° of the earlier calculations, but it was found that the alteration of the upper aft surface by the viscous ramp decreased the effective aft camber, lowering both the level of the under-pressures on the upper surface and the overpressures on the lower surface. The angle of attack was then simply increased to recover a match of the upper surface pressures. In Fig. 12 we show the resulting pressure distributions and the shape of the viscous ramp in terms of the slope distribution. The plus symbols on the aft upper surface denote the prescribed pressures. For this case the resulting shock at the surface represents a strong oblique shock where the downstream Mach number is subsonic. If we take the initial increment 5.1° as the wedge angle of the viscous ramp, then this is to be compared to 6.2° which would be required by the jump conditions to produce the shock pressure rise of the calculations for the calculated upstream Mach number of 1.28. This fair agreement is indeed encouraging though of course the use of a still finer mesh might have produced a more convincing result. There still remains however a difference in the lower surface pressures of Fig. 12 and experiments since the lower surface boundary layer displacement effects and the upper surface leading edge separation effects have not been taken into account in the calculation. The effect of the lower surface displacement effects would tend to decrease further the effective aft camber, further lowering both the upper surface under pressures and the lower surface over pressures. On the other hand leading edge separation would tend to decrease the suction levels over the upper surface as well as to produce the observed undulation in the supersonic pressures ahead of the shock. The net result must be that the angle of attack must be further changed to counterbalance these effects. If such effects could be calculated, then the difference of the resulting value of incidence and the geometric incidence in the experiment would then finally represent the incidence correction due to wall effects if such effects have not been sufficiently aggravated to invalidate a simple incidence correction. Needless to say viscous effects can play a complicating role even at high Reynolds numbers (though admittedly Airfoil A is an extreme profile), making a direct comparison of experiments and calculations a major undertaking.

In the above calculations the treatment of the "wake region" required an improvisation since the wake could not be simply treated as a rear stagnation streamline where a straightforward matching of the pressures and streamline

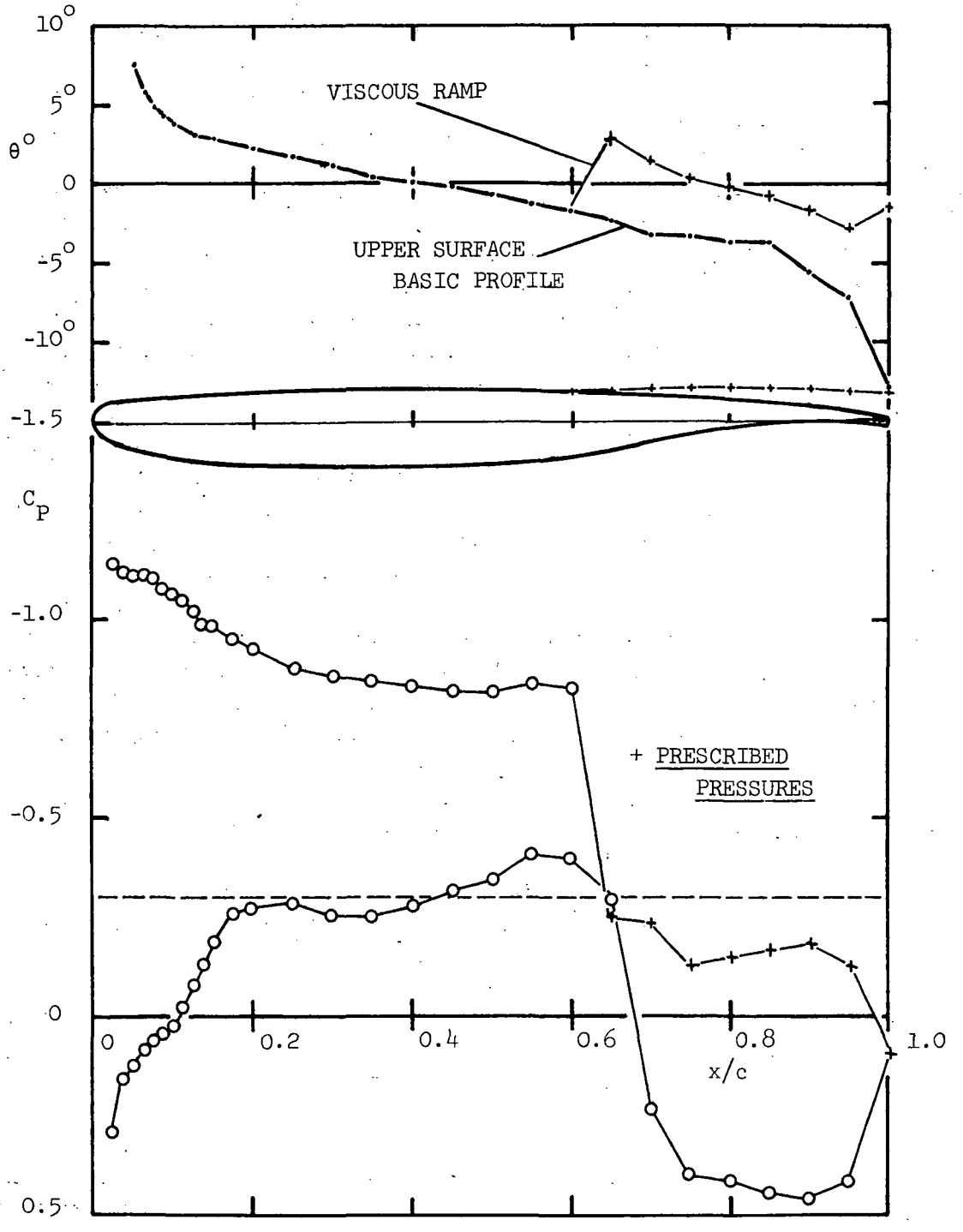

Figure 12. Viscous Ramp for Airfoil A at $M_\infty = 0.85$ and $\alpha = 2.4^\circ$

slopes was sufficient. Clearly across the wake a matching of the pressures is still a reasonably valid condition, but the streamline slopes clearly would not be equal. In the first attempt only a match of the pressures was used as a boundary condition on the sides of the slab representing the upper and lower surfaces of the wake. As probably should have been expected the calculations resulted in an instability in the wake region, suggesting the need for a second crossing relation analogous to the matching of the streamline slopes in the case of the rear stagnation streamline. Such a relation no doubt could be obtained by simultaneously calculating the wake flow, but in lieu of this, a jump condition in the streamline slopes across the wake was postulated as follows. First the slope of the centerline of the wake was prescribed to vary linearly from the average of the streamline slopes at the trailing edge to a zero value at a prescribed distance downstream of the trailing edge and then taken to be zero thereon downstream. The slope of the upper surface of the wake (actually the displacement surface) relative to the above meanline slope was then postulated to be positive and just the negative of the lower surface slope, again taken relative to the meanline. For high subsonic flows it would not be unreasonable to assume that the flow upstream of the trailing edge was relatively insensitive to the preciseness of the above postulated wake, though in the present calculation this insensitiveness was not verified.

Lastly as a further exercise in prescribing mixed conditions along the airfoil surface (either streamline slopes or pressures) we shall next investigate the possibility of evolving shockless flows or flows with weakened shocks by prescribing for example a continuous pressure distribution along the aft upper surface. Before we proceed to this task we note first some properties of shockless airfoil flows that severely limit what may be accomplished in this manner. First it is well known that along the sonic line (which is an isobar) the Mach waves "arriving" at the sonic line can only be expansion waves, while those "leaving" the sonic line must be compression waves. This then requires that only compression waves can impinge onto the airfoil surface, while only expansion waves can leave the surface when the flow is shockless. This requirement then mandates that the supersonic segment of the profile must have sufficient convexity to produce sufficient expansion effects to offset the effects of the incoming compression waves. Clearly, having any finite segment of zero curvature where the flow is supersonic would violate the above necessary condition for a shockless flow. Consider now the case of Airfoil A treated earlier. This airfoil has an upper surface having essentially zero curvature over much of the region where reduced convexity will be required, so it does not represent a promising candidate airfoil to render shockless. On the other hand it does represent an effective airfoil, and it

will be an interesting exercise to prescribe a continuous aft upper surface pressure distribution to see to what extent the shock wave can be weakened (or shortened). An approximate guide as to how far upstream the upper surface modification should be incorporated can be obtained by noting the approximate domain of dependence of the portions of the shock that are to be weakened. Thus in the case of Airfoil A at $M_\infty = 0.85$ and $\alpha = 1.4^\circ$ we shall prescribe an arbitrarily chosen continuous pressure distribution on the upper surface aft of the 30% chord station. The resulting pressure distribution and the shape of the resulting humping is shown in Fig. 13. Here the prescribed pressures are shown by the plus symbols. Shock weakening must be carried out only to an extent that the resultant drag in a real flow becomes just tolerable, since lift will be lost in the process of adding compression waves to the upper surface. In Fig. 14 we next show the resulting isobar pattern to illustrate the extent to which the shock has been weakened and shortened. Elimination of the stronger portions of the shock in the neighborhood of the surface not only reduces the entropy losses, but it also reduces significantly the adverse pressure gradients that would confront a boundary layer. In the above process a blunt base will invariably arise. Some bluntness of course is necessary to permit the removal of the boundary layer displacement effects, but in general further iterations in the shaping are required to evolve an aft upper surface configuration which does not produce adverse viscous effects.

Upper surface contouring to weaken the shock is not new, having been proposed earlier in Ref. 3 in the form of humped profiles. More recently Steger and Klineberg (Ref. 25) used the small disturbance steady relaxation procedure to calculate a number of interesting examples where also the surface pressures were prescribed either partially or entirely over the profile. Unavoidably the use of the small disturbance procedures can lead to numerical difficulties at the leading edge, especially in a lifting case, which seldom can be resolved in a satisfactory way. Several of the examples calculated by Steger and Klineberg were perhaps unacceptably compromised in the process of avoiding the leading edge problem by their assuming that the flow over and upstream of the nose remained invariant even when aft profile modifications produced a significant change in the lift.

In summary the results of the present section are gratifying in many respects and have yielded results that are reasonably viable. However it would be clearly premature to claim them to be "exact" inviscid results, since in no case was an assessment made of the effects of the remaining truncation errors. Particularly care must be exercised in the treatment of the shock where accuracy degrading diffusive damping must be employed to critically damp the

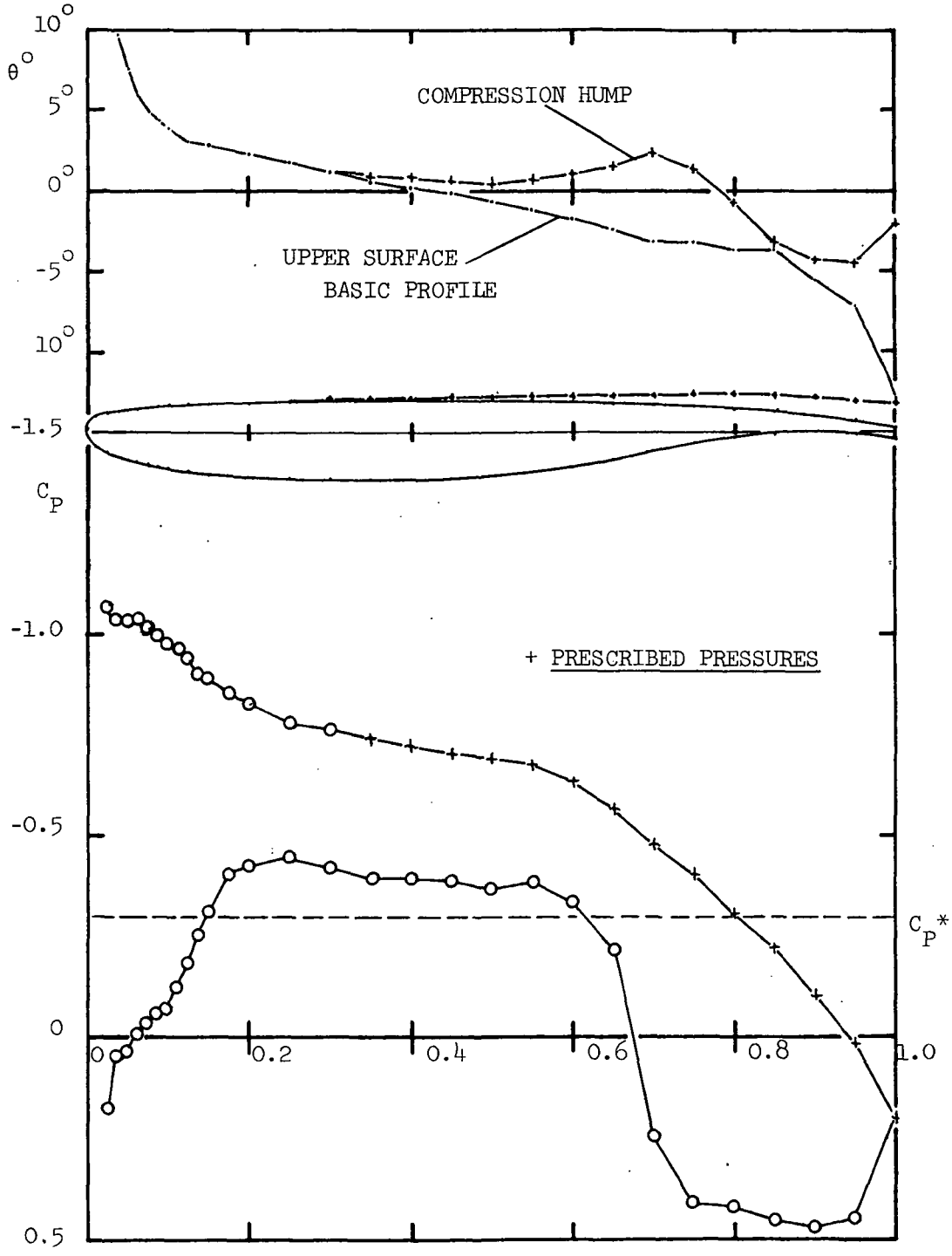

Figure 13. Example of the Weakened Shock Wave For Airfoil A at $M_\infty = 0.85$ and $\alpha = 1.4^\circ$

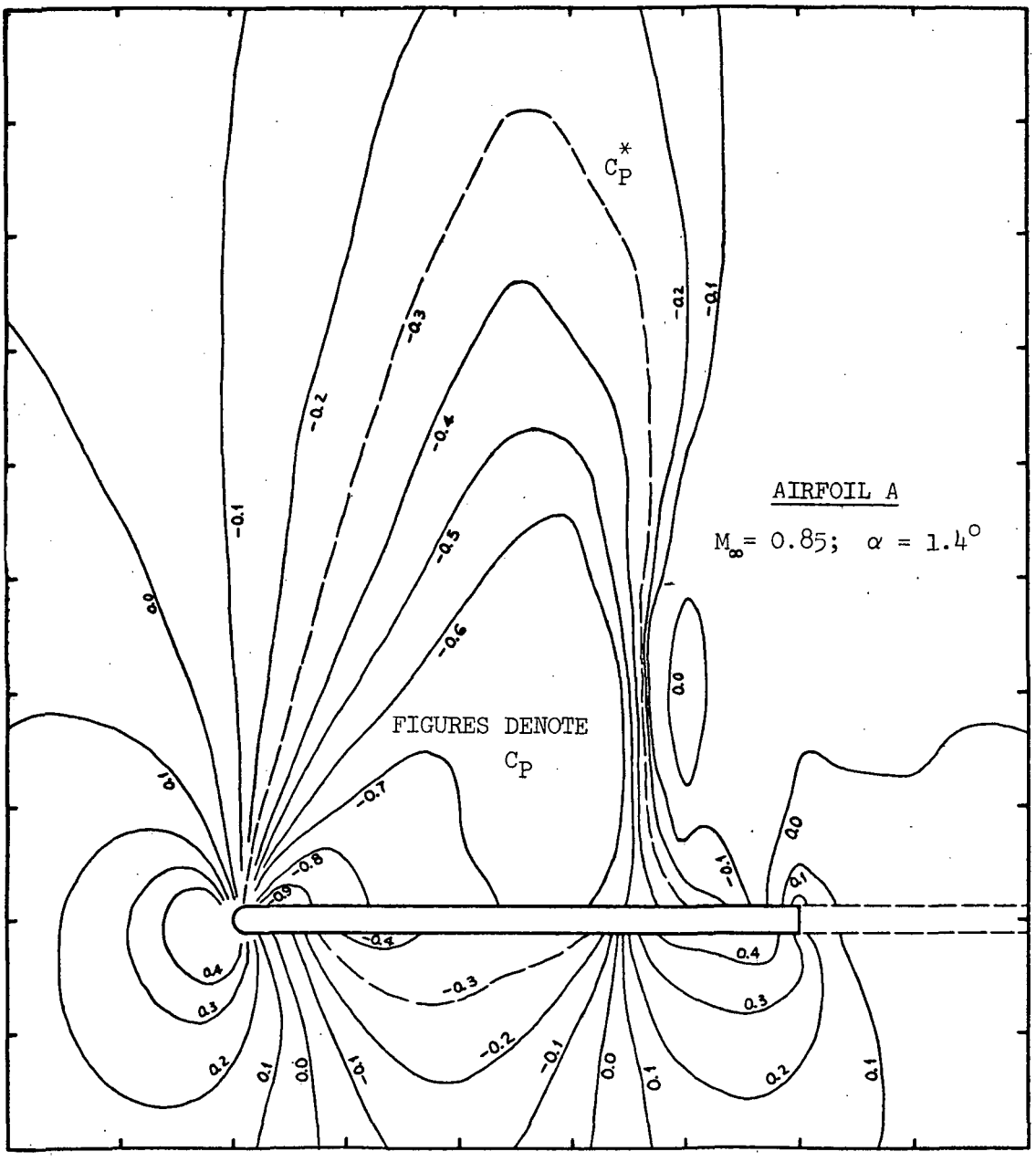

Figure 14. Isobars for Airfoil A With a Shock Attenuator Hump

over and under shoots about the shock that are characteristic with second order difference schemes. The Zierep post shock pressure cusp has features of an overshoot, so that it is essential that a sufficiently fine mesh be employed about the shock to capture the shock automatically and correctly when the oscillations are critically damped. Calculations on the whole are gradually becoming more routine, but despite the numerous examples computed to date, somehow annoying and time consuming surprises still manage to appear. Clearly we are still in the learning process.

Finally with regards to the computing time required, typically 300 seconds were required for a given case on the CDC 7600 computer using 4107 mesh points and 1500 time planes starting with an incompressible flow. Such times are an improvement over the original unsteady procedure and are tolerable for use in planar calculations, but clearly they are still intolerable for practical three dimensional examples.

6. CONCLUDING REMARKS

In the reported effort the flow was considered directly in the physical plane, since an important prerequisite for the finite difference analogue was its suitability for use in a procedure to incorporate viscous effects using a boundary layer concept, and for extension to steady three dimensional flows. Thus the use of the slab boundary and a quasi-planar condition along the parallel sides of the slab, introduced primarily to simplify the problem, are of particular convenience in applying profile modifications due to boundary layer displacement effects and for extension to three dimensional configurations.

The problem here was formulated as an unsteady (hyperbolic) problem with the equations expressed in appropriate conservation form in the subdomains containing shocks, to conform to the guidelines suggested by Lax that insure the proper jump conditions across the shock discontinuities. In contrast to this, in the steady formulation where the equations are of mixed elliptic-hyperbolic character, and additionally in some cases even of second order, the concept of a weak solution has not been established, and there simply is no guide, comparable to Lax's contributions, to pose the problem properly to insure proper shock jump conditions. Thus, for example, it is not clear whether, in the steady case, different shock jump conditions would result depending upon the form of the equations used as in the unsteady hyperbolic case. Here in the latter case as noted by Lax (Ref. 4) and Courant and Hilbert (Ref. 10), it may be recalled that even if the continuity and momentum equations are used in the identical conservation form, different shock con-

ditions are obtained if the fourth equation is expressed, not as the conservation of total enthalpy, but of entropy.

Quite apart from being able to define a weak solution, there is still the task of obtaining the thus-defined weak solution by a numerical procedure. Here again we are indebted to Lax who has shown that, at least for an initial value problem, the proper weak solution can be obtained by solving a properly posed finite difference problem. The results of the present calculations indicate that Lax's conclusion can be extrapolated to the more complex airfoil problem, where the proper shock jump conditions and Zierep's post-shock expansion (we shall discuss this later) can be obtained when a sufficiently fine mesh about the shock is used.

To review the situation for the treatment of the shock, in Fig.15 we have plotted the values of M_2^* (based upon a^*) at the airfoil surface downstream of the shock as a function of the values upstream for both the unsteady calculations (Ref. 3 and the present results) as well as the steady relaxation calculations (Refs. 6, 7, 17, 18, 24). Also shown are the curves reflecting the jump conditions implied by the unsteady weak solutions, as well as those from the Rankine-Hugoniot conditions consistently approximated. Consider first the unsteady results. The results of the present calculations as noted earlier do indeed fulfill the expected jump conditions, while the earlier results of Ref. 3 exhibit a scatter, and in most cases the values of M_2^* are somewhat below the correct values. These latter discrepancies can be eliminated by simply decreasing the excessive diffusive damping which has caused a round off of the Zierep cusped pressure bucket as was demonstrated in an example of Section 5. (See also Fig.15). On the other hand the steady relaxation results have a significantly greater scatter, and the implied mean curves fall considerably below the corresponding Rankine-Hugoniot values. Most probably the scatter is due in great part to an inadequate mesh spacing, since the use of the potential rather than the velocities as the dependent variable would make more stringent the requirements on the mesh size. However the cause of the large departures from the desired shock jump conditions remaining after the scatter is eliminated is uncertain at present. Though such a departure could be caused either by the excessive damping effects rounding off the Zierep cusped pressure bucket as in the unsteady case described earlier, or possibly to the form of the equations implying jump conditions other than the desired ones, it is also possible that the cause may be due to an inadequacy in the numerical procedure itself where only a dichotomy of difference schemes is employed to represent a continuous variation of the "domain of dependence." In other words it may be conjectured that the flow is "shocked" not by the physics, but by the abrupt change in the difference scheme. Under these

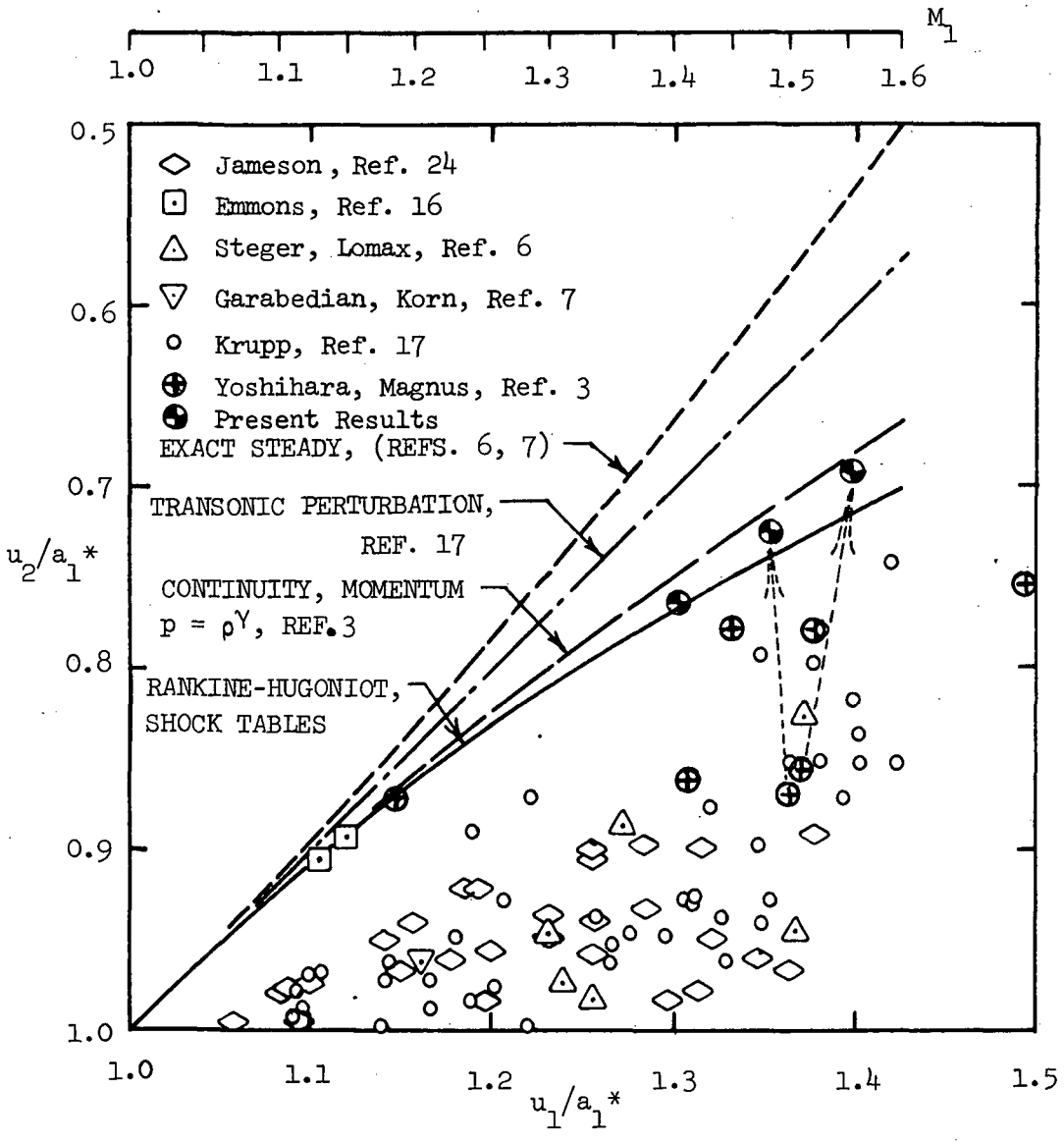

Figure 15. Velocity Jump at Shock Ending Supersonic Region on Airfoil

conditions it would be unreasonable to expect the correct jump conditions. Clearly the picture would be clarified by carrying out additional calculations with refined mesh schemes. Thus at the present stage one must hold in abeyance the shock-capturing ability of the steady relaxation procedures. If a refined mesh does not remedy the situation, one should seriously consider a modification of the procedure to fit in a shock discontinuity directly, imposing the shock jump conditions, as was done earlier by Emmons (Refs. 16 and 17), whose results (Fig. 7, Ref. 17) as shown in Fig.15 do indeed fulfill the required jump conditions. With such a modification the resulting steady relaxation procedures, especially those where the airfoil is mapped into a circle, would be difficult to improve upon from the point of view of both accuracy and computor costs.

In summary with regard to the treatment of the shocks, the unsteady finite difference analogue as used is based upon a reasonably sound mathematical background, and the results show that the proper shock jump conditions are fulfilled, and hence the correct shock location should then follow. On the other hand the steady relaxation procedures must await further effort before the treatment of shocks can be credibly accepted. Here, in the absence of a reliable guide for the correct formulation of the numerical analogue to assure the proper capturing of the shock, one should seek instead means to fit explicitly a shock discontinuity into the flow using the proper jump conditions across the shock.

The discussions above regarding the surface shock pressure rise pertain to inviscid flow. These inviscid results are seldom observed in technically important experiments due to the interaction of the shock wave with the boundary layer, which in cases of interest is fully turbulent upstream of the shock. As the consequence of the interaction either an abrupt thickening or a separation of the boundary layer takes place at the foot of the shock, and the resulting displacement effect of the boundary layer changes the shock at the surface from a normal shock in the inviscid case, to an oblique shock leading to a decreased pressure rise across the shock. Since the location of the shock is in part dependent upon the shock pressure rise, as well as the nature of the subsonic pressure recovery downstream of the shock, it is of paramount importance to develop a procedure to treat the above viscous interactions. In Ref. 20 a procedure has been suggested not only to evolve a fully determined system of turbulent boundary layer equations in the Von Karman integral format to treat a separated boundary layer, but also to solve the strong viscid-inviscid flow coupling. Here the artifice of a wedge-shaped viscous ramp has been introduced to simulate the boundary layer displacement effects.

In determining the surface shock pressure rise from experiments, in particular where there is negligible boundary layer thickening downstream of the shock, one must keep in mind the possible presence of an abrupt post shock expansion measured by Ackeret, Feldmann, and Rott (Ref. 21) and deduced by Emmons (Ref. 16). If the pressure taps on the model are insufficiently spaced, then such an expansion can be overlooked, and an erroneous pressure rise can be inferred by an improper interpolation of the measured pressures.

The behavior of the flow at the foot of the shock has been analyzed by Zierep (Ref. 22) and by Ferrari (Ref. 23) by a local analysis about the foot of the shock. For convex surfaces they found that the shock curvature was logarithmically infinite at the surface, the shock changing from a normal shock at the surface to an oblique shock at an infinitesimal distance off of the surface, and that an abrupt expansion occurred just downstream of the shock (in fact starting with an infinite gradient). The uniqueness of such local singular solutions, as pointed out by Ferrari, is difficult to establish, but the measurements of Ackeret as well as some existing calculations do indeed exhibit the principal features deduced by Zierep. On the other hand the local analysis does not of course establish the scale of the cusped pressure bucket, both in terms of its depth as well as its width, so that if these scales are sufficiently small, then it is conceivable that a finite difference result can satisfactorily capture the shock without exhibiting a pressure bucket. When a significant pressure bucket does arise, the extent that it can be captured by a finite difference calculation would depend upon the mesh size used, since the truncation errors lead to dissipative effects which tend to round off the cusp. In the case that the airfoil surface at the base of the shock has zero curvature or a concave curvature as in the viscous case with a viscous wedge such a post-shock expansion would not necessarily arise. (Clearly such a post-shock expansion does not arise in the case of a detached shock ahead of a symmetric wedge at zero incidence at slightly supersonic M_∞).

In the inviscid steady relaxation calculations erroneous shock pressure rises (see Fig. 15) have been obtained that are reasonably close to those that would be expected in experiments with the viscous effects present. It is highly tempting to then suggest that viscous effects need not be incorporated, especially since a viable viscous procedure has not yet been demonstrated. There are two fallacies inherent in such a point of view. First of all it is not assured by any means that the proper shock location would be obtained even with the use of the pseudo-shock, since the reduced shock pressure rise would be in error off the surface, and it is not accompanied by the proper shock obliqueness at the surface. Perhaps of more importance is the fact that the boundary layer displacement effects, essential in determining the effective

airfoil camber, would not be accounted for in such an approach; and it is well known that a change of the effective camber, especially in an aft-cambered airfoil, can affect the entire pressure distribution. On the other hand the results using the steady relaxation procedure with its pseudo-shock undoubtedly yield surface pressure distributions in most cases that are closer to the experimental results than the inviscid results with a true shock. The steady inviscid relaxation procedures therefore would serve as a valuable predesign tool even if viable boundary layer procedures were eventually developed.

In closing the authors wish to express their appreciation to Mr. Ralph Carmichael, who served as the NASA contract monitor, for his enthusiastic support and assistance during the present study, particularly during the post midnight sessions associated with time-sharing computors.

7. REFERENCES

1. Magnus, R.; Gallaher, W.; and Yoshihara, H.: Inviscid Supercritical Airfoil Theory. AGARD CP No. 35, 1968.

2. Magnus, R.; and Yoshihara, H.: Inviscid Transonic Flow Over Airfoils. AIAA Journal, Vol. 8, No. 12, Dec. 1970, pp. 2157-2162.

3. Yoshihara, H.; and Magnus, R.: A Search for Improved Transonic Profiles. General Dynamics/Convair, GDC-ERR-1536, May 1970.

4. Lax, P.: Weak Solutions of Nonlinear Hyperbolic Equations and Their Numerical Computation. Comm. on P. and Appl. Math., Vol. VII, 1954.

5. Murman, E.; and Cole, J.: Calculation of Plane Steady Transonic Flows. AIAA Journal, Vol. 9, No. 1, Jan. 1971, pp. 114-121.

6. Steger, J.; and Lomax, H.: Transonic Flow About Two Dimensional Airfoils by Relaxation Procedures. AIAA Journal, Vol. 10, No. 1, Jan. 1972, pp. 49-54.

7. Garabedian, P.; and Korn, D.: Analysis of Transonic Airfoils. Communications on Pure and Applied Mathematics, Vol. 24, 1971, pp. 841-851.

8. Yoshihara, H.: Some Recent Developments in Planar Inviscid Transonic Airfoil Theory. AGARDograph AG-156, 1972.

9. Grossman, B.; and Moretti, G.: Time-Dependent Computations of Transonic Flows. AIAA Paper 70-1322, Oct. 1970.

10. Courant, R.; and Hilbert, D.: Methods of Mathematical Physics, Vol. II. Interscience Publishers, New York, 1962, pp. 486-490, and 635-36.

11. Magnus, R.: Research on Numerical Analysis of Transonic Flowfields. General Dynamics/Convair GDC-ERR-1608, Dec. 1970.

12. Guderley, G.: Theorie Schallnaher Strömungen. Springer Verlag, Berlin, 1957, pp. 32-43.

13. Richtmyer, R.: A Survey of Difference Methods for Non-Steady Fluid Dynamics. Nat. Center for Atm. Research Report NCAR TN 63-2, 1962.

14. Magnus, R.; and Yoshihara, H.: Research on Unsteady Transonic Flow Theory. General Dynamics/Convair Report No. CM 72-2032, 1972.

15. Yoshihara, H.; Zonars, D. (AFFDL); and Carter, W.: High Reynolds Number Transonic Performance of Advanced Planar Airfoils with Jet Flaps. AFFDL-TR-71-61, June 1971.

16. Emmons, Howard N.: The Numerical Solution of Compressible Fluid Flow Problems. NACA TN 932, May 1944.

17. Emmons, Howard W.: Flow of a Compressible Fluid Past a Symmetrical Airfoil in a Wind Tunnel and in Free Air. NACA TN 2746, Nov. 1948.

18. Krupp, James A.: The Numerical Calculation of Plane Steady Transonic Flows Past Thin Lifting Airfoils. Boeing Scientific Research Laboratories, D180-23958-1, June 1971.

19. Krupp, J. A.; and Murman, E.M.: The Numerical Calculation of Steady Transonic Flows Past Thin Lifting Airfoils and Slender Bodies. AIAA Paper 71-566, June 1971.

20. Yoshihara, H.; Magnus, R.; and Fatta, J.: Strong Boundary Layer-Shock Wave Interactions on Airfoils - An Exploratory Study. General Dynamics/Convair Report GDC-ERR-1702, 1972.

21. Ackeret, J.; Feldmann, F.; and Rott, N.: Investigations of Compression Shocks and Boundary Layers in Gases Moving at High Speeds. NACA TM No. 1113, 1947.

22. Zierep, J.: Der senkrechte Verdichtungsstoss am Gekrümmten Profil. ZAMP Vol. IXb, 2958, pp. 764-776.

23. Ferrari, C., and Tricomi, F., Transonic Aerodynamics, Academic Press, New York, 1968, pp. 346-364.

24. Jameson, A.: Transonic Flow Calculations for Airfoils and Bodies of Revolution. Grumman Report 390-71-1, 1971.

25. Steger, J., and Klineberg, J.: A Finite Difference Method for Transonic Airfoil Design. AIAA Preprint No. 72-679, 1972.

NASA-Langley, 1973 —— 1

"The aeronautical and space activities of the United States shall be conducted so as to contribute . . . to the expansion of human knowledge of phenomena in the atmosphere and space. The Administration shall provide for the widest practicable and appropriate dissemination of information concerning its activities and the results thereof."

—NATIONAL AERONAUTICS AND SPACE ACT OF 1958

NASA SCIENTIFIC AND TECHNICAL PUBLICATIONS

TECHNICAL REPORTS: Scientific and technical information considered important, complete, and a lasting contribution to existing knowledge.

TECHNICAL NOTES: Information less broad in scope but nevertheless of importance as a contribution to existing knowledge.

TECHNICAL MEMORANDUMS: Information receiving limited distribution because of preliminary data, security classification, or other reasons. Also includes conference proceedings with either limited or unlimited distribution.

CONTRACTOR REPORTS: Scientific and technical information generated under a NASA contract or grant and considered an important contribution to existing knowledge.

TECHNICAL TRANSLATIONS: Information published in a foreign language considered to merit NASA distribution in English.

SPECIAL PUBLICATIONS: Information derived from or of value to NASA activities. Publications include final reports of major projects, monographs, data compilations, handbooks, sourcebooks, and special bibliographies.

TECHNOLOGY UTILIZATION PUBLICATIONS: Information on technology used by NASA that may be of particular interest in commercial and other non-aerospace applications. Publications include Tech Briefs, Technology Utilization Reports and Technology Surveys.

Details on the availability of these publications may be obtained from:

SCIENTIFIC AND TECHNICAL INFORMATION OFFICE

NATIONAL AERONAUTICS AND SPACE ADMINISTRATION

Washington, D.C. 20546